Cell Stress and Chaperones (2024) 29:567–588
https://doi.org/10.1016/j.cstres.2024.06.001

Mild heat shock at 40 °C increases levels of autophagy: Role of Nrf2

Mélanie Grondin · Claire Chabrol · Diana A. Averill-Bates*

Received: 30 May 2024 / Revised: 7 June 2024 / Accepted: 9 June 2024

Abstract

The exposure to low doses of stress induces an adaptive survival response that involves the upregulation of cellular defense systems such as heat shock proteins (Hsps), anti-apoptosis proteins, and antioxidants. Exposure of cells to elevated, non-lethal temperatures (39–41 °C) is an adaptive survival response known as thermotolerance, which protects cells against subsequent lethal stress such as heat shock (> 41.5 °C). However, the initiating factors in this adaptive survival response are not understood. This study aims to determine whether autophagy can be activated by heat shock at 40 °C and if this response is mediated by the transcription factor Nrf2. Thermotolerant cells, which were developed during 3 h at 40 °C, were resistant to caspase activation at 42 °C. Autophagy was activated when cells were heated from 5 to 60 min at 40 °C. Levels of acidic vesicular organelles (AVOs) and autophagy proteins Beclin-1, LC3-II/LC3-I, Atg7, Atg5, Atg12–Atg5, and p62 were increased. When Nrf2 was overexpressed or depleted in cells, levels of AVOs and autophagy proteins were higher in unstressed cells, compared to the wild type. Stress induced by mild heat shock at 40 °C further increased levels of most autophagy proteins in cells with overexpression or depletion of Nrf2. Colocalization of p62 and Keap1 occurred. When Nrf2 levels are low, activation of autophagy would likely compensate as a defense mechanism to protect cells against stress. An improved understanding of autophagy in the context of cellular responses to physiological heat shock could be useful for cancer treatment by hyperthermia and the protective role of adaptive responses against environmental stresses.

Keywords Heat shock · Adaptive survival response · Autophagy · Nrf2 · Thermotolerance

Abbreviations: AFC, 7-amino-4-trifluoromethylcoumarin; Ambra1, activating molecule in Beclin 1-regulated autophagy; AMC, 7-amino-4-methylcoumarin; AMP, Adenosine monophosphate; AMPK, 5' AMP-activated protein kinase; Atg, autophagy-related genes; AVO, acidic vesicular organelle; ATP, Adenosine triphosphate; Bif-1, endophilin B1/Bax-interacting factor 1; BSA, bovine serum albumin; cDNA, complementary DNA; CHAPS, 3-[(3-cholamidopropyl) dimethylammonio]-1-propanesulfonate; DAPI, 4',6-diamidino-2-phenylindole; DEVD, Asp-Glu-Val-Asp; DGR, glycine repeat domains; DMEM, Dulbecco modified Eagle's medium; DNA, Deoxyribonucleic acid; DTT, dithiothreitol; EDTA, ethylene diamine tetraacetic acid; EGTA, ethylene glycol tetraacetic acid; FBS, fetal bovine serum; GAPDH, glyceraldehyde 3-phosphate dehydrogenase; GCL, gamma cysteine ligase; H_2O_2, hydrogen peroxide; HeLa, cervical carcinoma cell line; HO-1, heme oxygenase-1; HSF1, heat shock factor 1; Hsp, heat shock protein; Inh, inhibitor; KD, knockdown; Keap1, Kelch ECH associating protein1; LC3, microtubule-associated protein 1 A/1B-light chain 3; LEHD, Leu-Glu-His-Asp; LTR, LysoTracker; MnSOD, manganese superoxide dismutase; MOPS, 3-morpholinopropane-1 sulfonic acid; mRNA, messenger RNA; mTOR, mammalian target of rapamycin; N, normal, non-thermotolerant cells; NaCl, Sodium chloride; NF-κB, nuclear factor kappa-light-chain-enhancer of activated B cells, PBS, phosphate buffered saline; Nrf2, nuclear factor erythroid 2-related factor 2; OE, overexpression; pAMPK, phosphorylated AMP-activated protein kinase; PE, phosphatidylethanolamine; PI3K, phosphatidylinositol 3-kinase; PIPES, 1,4-piperazinediethanesulfonic acid; PMSF, phenylmethylsulfonyl; qRT-PCR, quantitative real-time polymerase chain reaction; RNA, Ribonucleic acid; rRNA, ribosomal RNA; Rubicon, RUN domain protein as Beclin 1 interacting and cysteine-rich containing; SDS-PAGE, sodium dodecyl sulfate-polyacrylamide gel electrophoresis; SEM, Standard Error of the Mean; ULK1/2, unc-51-like autophagy-activating kinases 1/2; UVRAG, UV radiation resistance-associated gene; Vps-34, vacuolar protein sorting-34

* Diana A. Averill-Bates
averill.diana@uqam.ca

Département des Sciences Biologiques, Centre d'Excellence en Recherche sur les Maladies Orphelines – Fondation Courtois (CERMO-FC), Faculté des Sciences, Université du Québec à Montréal, Montréal, Québec, Canada.

Published online: 14 June 2024

Introduction

Hyperthermia is a promising modality for cancer treatment as an adjuvant to chemotherapy and/or radiotherapy.[1] For clinical hyperthermia, temperatures in the range of 40–44 °C can be targeted to a localized area of the body that has been invaded by a tumor.[2] Hyperthermia sensitizes cells to radiation and chemotherapy, and the tumor-targeting approach allows for increased therapeutic efficacy without increasing their toxic side effects to normal tissues.[1–6]

Heat is one of the most potent radiosensitizers known.[2,7–9] Cells in the S phase of the cell cycle and hypoxic cells at the center of solid tumors are resistant to radiation. However, S-phase cells are heat-sensitive. In addition, the low pH environment of solid tumors increases heat sensitivity, which allows radio-resistant hypoxic cells to become radiosensitive. Moreover, hyperthermia improves tumor oxygenation, increases tumor blood flow,[10] and inhibits the repair of radiation-induced DNA damage.[1] Heat increases the cytotoxic effects of a variety of chemotherapeutic agents. In addition, heat at temperatures of 39–43 °C improved vasodilation, which allows for increased drug delivery to the tumor due to increased blood flow and increased vascular permeability.[1] Another beneficial effect of hyperthermia for cancer treatment is the ability to modulate both innate and adaptive immune responses.[11]

In clinical trials, the use of hyperthermia in combination with chemotherapy and/or radiotherapy has led to improved outcomes for multiple tumor sites. These include cervix, head and neck, breast, lung, bladder, melanoma, pancreas, soft tissue sarcoma, esophagus, liver, prostate, rectum, and glioblastoma.[1–6,8,12] Regardless of the promising clinical results, the cellular and molecular mechanisms involved in heat responses have not been fully delineated.[13,14]

Temperatures of 41.5 °C and higher are cytotoxic, and this response increases as the temperature rises. However, when cells are exposed to lower, non-lethal temperatures (39–41 °C), they develop thermotolerance.[15–17] Thermotolerant cells are resistant to subsequent cytotoxic insults such as heat shock[15,16,18,19] and oxidative stress.[20] Traditionally, thermotolerance has been associated with the accumulation of heat shock proteins (Hsps).[15–19,21]

Nuclear factor erythroid 2-related factor 2 (Nrf2) is a transcription factor that regulates the antioxidant response.[22,23] Under normal conditions, Nrf2 remains inactive in the cytosol through binding to its repressor protein Kelch ECH associating protein 1 (Keap1), which mediates its degradation by the proteasome.[22,24] However, under oxidizing conditions or stress, the cysteine groups of Keap1 are altered, and Nrf2 is released, which allows it to accumulate. Nrf2 undergoes phosphorylation and translocation to the nucleus.[24,25] Once in the nucleus, Nrf2 binds to small Maf proteins and the antioxidant response element (ARE),[26] where it upregulates the transcription of hundreds of genes for cellular defense molecules and proteins, including antioxidants, detoxifying enzymes, metabolic enzymes, and stress response proteins.[22,23]

Autophagy is another cell survival response that orchestrates the intracellular degradation of damaged molecules and organelles.[27,28] Macroautophagy entails the sequestration of cellular materials destined for degradation in double-membrane vesicles called autophagosomes, which fuse with lysosomes to form autolysosomes that degrade and recycle these materials.[27,29] Autophagy is regulated by several autophagy-related genes (*atg*) and the proteins they encode.[28–31] The elongation phase and completion of the autophagosomal membrane involve two conjugation systems: (i) the Atg12–Atg5–Atg16L and (ii) the Atg8-microtubule-associated protein 1A/1B-light chain 3 (LC3)–phosphatidylethanolamine conjugation systems.[28,29,32]

Thermotolerance developed at mild temperatures such as 40 °C constitutes a hormetic, adaptive cell survival response that is associated with increased accumulation of Hsps.[17,21] However, in addition to Hsps, we reported that levels of other cellular defense molecules, namely antioxidants, endoplasmic reticulum (ER) stress proteins, and Nrf2, were increased in cells that were preconditioned at a mild temperature of 40 °C.[20,21,33,34] Although hyperthermia is a promising treatment for cancer, thermotolerance induced at non-lethal temperatures can lead to thermoresistance due to increased levels of defense molecules such as Hsps, antioxidants, Nrf2, and ER stress proteins. This adds a layer of complexity to the heat shock response induced at mild temperatures and indicates that further studies are required to fully understand this phenomenon, in particular to mitigate thermoresistance during hyperthermia treatments. In addition, links between Nrf2 and autophagy have been reported and occur through the autophagy receptor protein p62 and the Nrf2 repressor protein Keap1.[35–37] The role of autophagy during the development of an adaptive stress response by mild heat at 40 °C is not known.

This study aims to improve understanding of mechanisms involved in the activation of protective cellular defenses during a hormetic, adaptive cell survival response induced by mild heat shock at 40 °C. It is likely that additional cellular defense processes could be involved in this adaptive, mild heat shock response. Therefore, we investigate whether the cell survival process autophagy could play a role in this adaptive survival response induced by mild, non-lethal heat

shock at 40 °C. Given that there are established links between autophagy and Nrf2,[35,38] we determine if Nrf2 could alter cellular responses to autophagy at 40 °C. This work aims to improve understanding of mechanisms that are relevant to clinical hyperthermia treatment, cancer biology, and the protective role of adaptive responses against toxic, environmental stresses.

Results

Mild heat shock at 40 °C protects cells against heat stress-induced apoptosis

We evaluated whether preconditioning of cells at 40 °C can protect cells against heat-induced cell death. When HeLa cells were heated at 42 °C, there was a significant increase in the activity of caspase-3 after 2–3 h (Figure 1(A)) and caspase-9 after 1–2 h (Figure 1(B)). Heating of cells from 30 min to 3 h at 42 °C caused a significant loss of viability (Figure 1(C)) and a significant increase in levels of apoptosis (Figure 1(D)). Levels of necrotic cells at 42 °C were low at less than 5% (Figure 1(D)). The preconditioning of cells at 40 °C for 3 h rendered them partially resistant to apoptosis induced by heat shock at 42 °C (Figure 1). Caspase-3 and caspase-9 activation (Figure 1(A) and (B)) and cell death (Figure 1(D)) were diminished significantly in thermotolerant cells, compared to normal, control cells that were maintained at 37 °C for 3 h. Further, the loss of viability at 42 °C was partially reversed in thermotolerant cells (Figure 1(C)). Levels of necrosis in cells heated at 42 °C were low in thermotolerant cells (< 5%) (Figure 1(D)).

We subsequently verified if heating cells at 40 °C can cause cell death (Figure 2). When cells were heated at 40 °C for times up to 2 h, there was no activation of caspase-3 (Figure 2(A)) or caspase-9 (Figure 2(B)), whereas there was significant activation of these two caspases at 42 °C. There was a small loss of viability (< 10%) at 40 °C, compared to a larger, significant

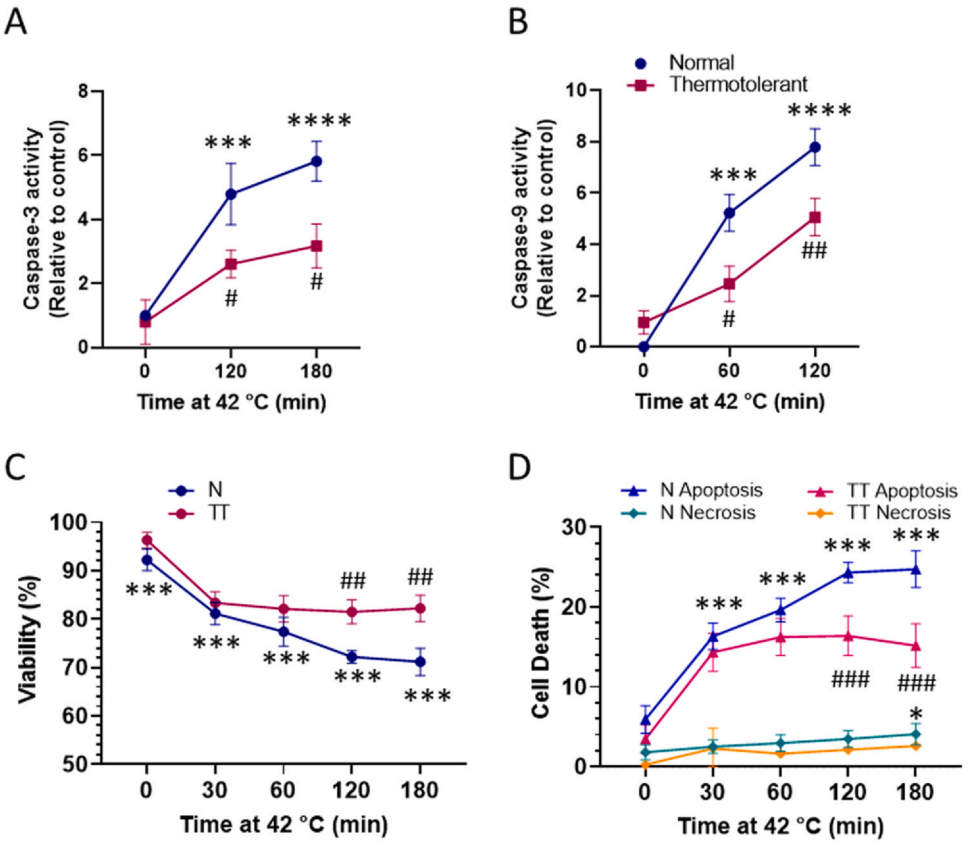

Fig. 1 Protective effect of preconditioning at 40 °C against cell death induced by heat shock at 42 °C. Normal (N, non-thermotolerant) and thermotolerant (TT) HeLa cells were heated at 42 °C from 0 to 120 or 180 min. Activities of caspase-3 (A) and caspase-9 (B) were relative to unheated controls (time = 0 min at 42 °C, 1.0). Viability (C) was relative to unheated normal controls (time = 0). Percent apoptotic and necrotic cells was relative to total cells (100%) (D). Data represent mean ± standard error of the mean (SEM) from five independent experiments. (***) $P < 0.0005$; (****) $P < 0.0001$: significant difference between unheated control (T = 0) and normal cells heated at 42 °C. (#) $P < 0.05$; (##) $P < 0.005$; (###) $P < 0.0005$: significant difference between normal and thermotolerant cells for each treatment time.

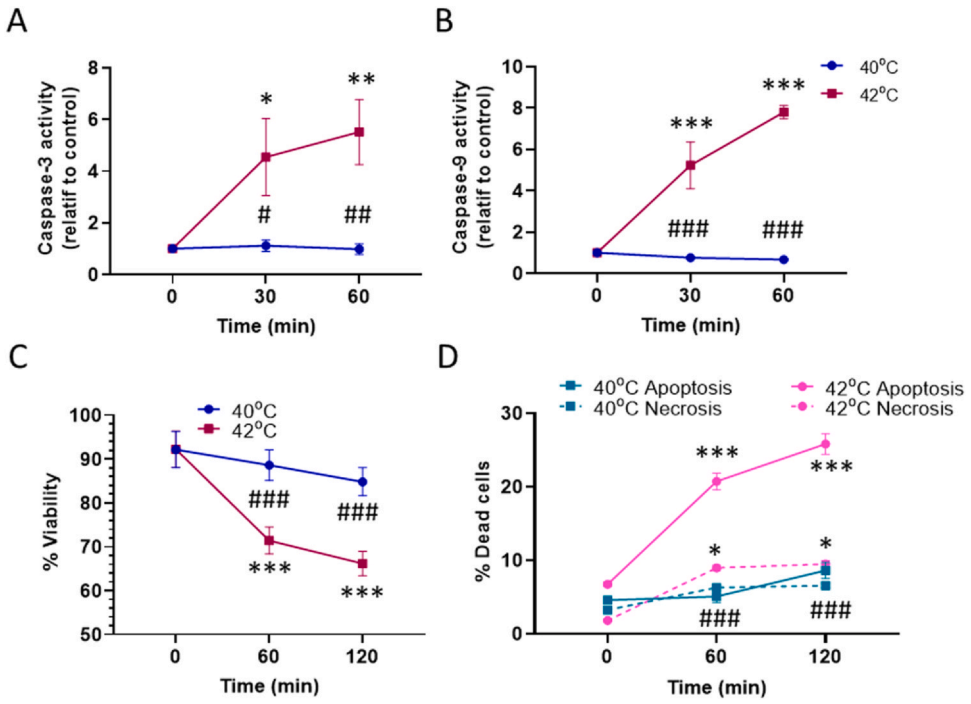

Fig. 2 Comparison of levels of cell death during heating at 40 and 42 °C. Normal (N, non-thermotolerant) HeLa cells were heated at 40 or 42 °C from 0 to 2 h. Activities of caspase-3 (A) and caspase-9 (B) were relative to unheated controls (time = 0 min at 40 °C, 1.0). Data represent mean ± SEM from four independent experiments. Viability (C) was relative to unheated controls (time = 0). Percent apoptotic and necrotic cells (D) was relative to total cells (100%). Data represent mean ± SEM from five independent experiments. (*) $P < 0.5$; (**) $P < 0.005$; (***) $P < 0.0005$: significant difference between unheated control (T = 0) and normal cells heated at 42 °C. (#) $P < 0.05$; (##) $P < 0.005$; (###) $P < 0.0005$: significant difference between cells heated at 40 °C *versus* 42 °C for each treatment time.

decrease (< 30%) at 42 °C (Figure 2(C)). Levels of apoptotic and necrotic cells were low (< 5%) at 40 °C, whereas apoptosis was significantly induced at 42 °C (Figure 2(D)). These results show that heat treatment at 40 °C for up to 2 h was a preconditioning treatment that was non-toxic.

Mild heat shock at 40 °C increases Nrf2 levels

To look for activation of early cell survival responses during a preconditioning heat treatment at 40 °C, short exposure times were used from 15 to 60 min. The transcription factor Nrf2 has been implicated as a central and underlying mechanism of hormesis.[39] Cells with knockdown (KD) or overexpression (OE) of Nrf2 were prepared using CRISPR-Cas9. In cells overexpressing Nrf2, protein levels of Nrf2 were increased significantly by 3.12-fold using Western blotting (Figure 3(A) and (B)) and by 6-fold using qRT-PCR (Figure 3(C)), relative to wild type (WT) control cells. For Nrf2 KD cells, protein levels of Nrf2 decreased significantly by 72% (Figure 3(A) and (B)) and mRNA levels by about 50% (Figure 3(C)). The significant decrease in Nrf2 levels in KD cells and increase in OE cells were also visible by fluorescence microscopy (Figure 3(I) and (J)). Messenger ribonucleic acid (mRNA) levels of Nrf2 targets such as catalase (Figure 3(D)), manganese superoxide dismutase (MnSOD) (Figure 3(E)), heme oxygenase-1 (HO-1) (Figure 3(F)), gamma cysteine ligase (GCL) (Figure 3(G)), and Hsp72 (Figure 3(H)) were significantly decreased in Nrf2 KD cells, compared to WT cells. On the other hand, levels of these Nrf2 targets were significantly higher in Nrf2 OE cells than in controls (Figure 3(D)–(H)).

Subsequently, cellular Nrf2 levels were evaluated during mild heat shock at 40 °C. Nrf2 levels were detected by fluorescence microscopy and increased significantly when cells were heated for 30–60 min at 40 °C (Figure 3(I) and (J)). These results show that Nrf2 is activated as an early response to mild heat shock at 40 °C. Levels of Nrf2 in KD cells were significantly lower than in WT cells and did not change during heating at 40 °C (Figure 3(I) and (J)). In OE cells, Nrf2 levels were high in unheated controls and increased further after 30–60 min at 40 °C (Figure 3(I) and (J)). Nrf2 was present in the nucleus in WT and OE cells, which indicated that Nrf2 was activated under these conditions (Figure 3(I)).

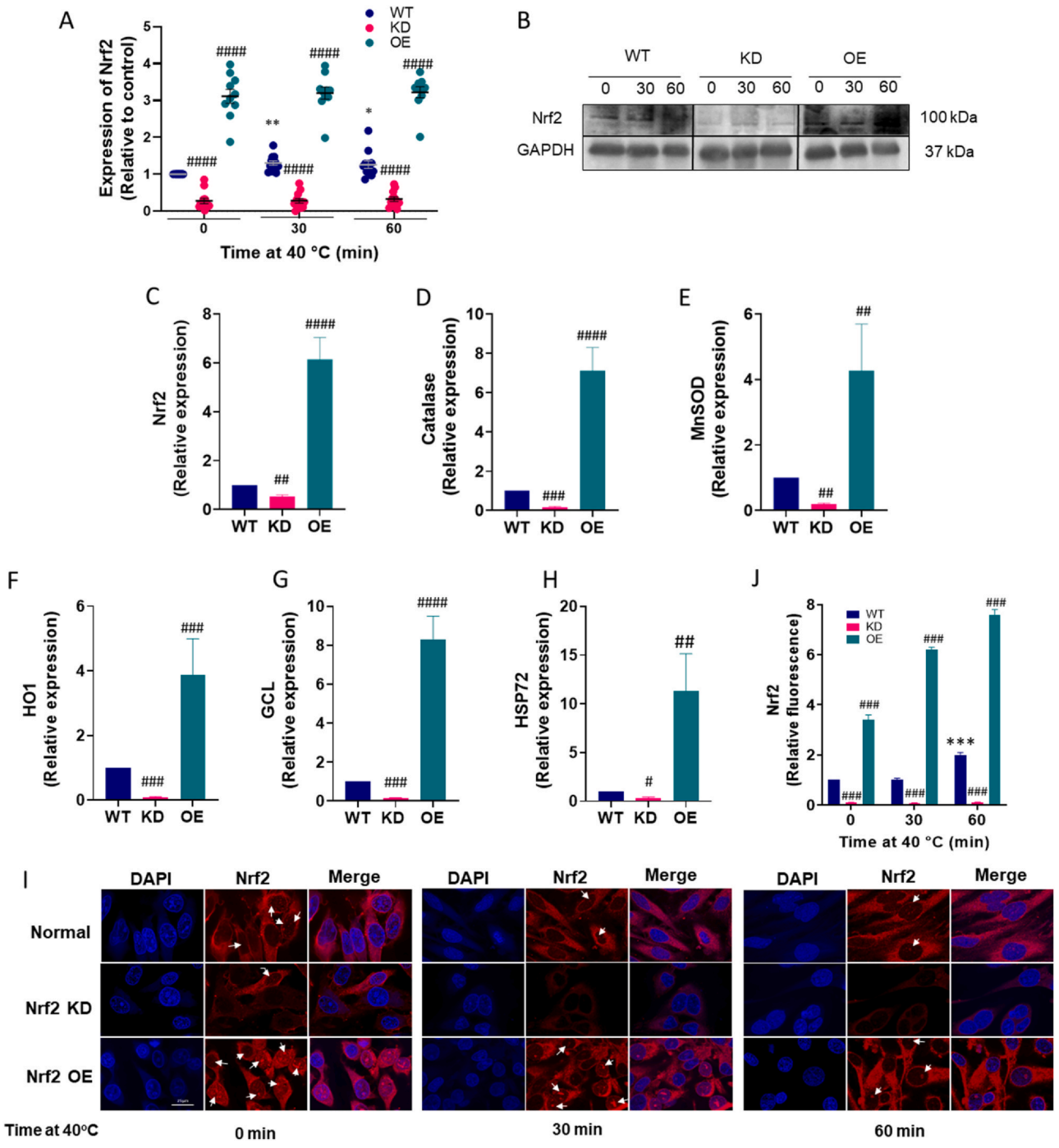

Fig. 3 Characterization of cell lines with altered Nrf2 expression. Protein expression of Nrf2 was determined by Western blotting in KD and OE cells, compared to WT cells (1.0) using a glyceraldehyde 3-phosphate dehydrogenase (GAPDH) loading control from the same membrane (A and B). mRNA expression of Nrf2 (C), catalase (D), MnSOD (E), HO-1 (F), GCL (G), and Hsp72 (H) was determined by qRT-PCR in KD and OE cells, relative to WT cells (1.0). Nrf2 levels (I) were determined by confocal microscopy (60×) using an Alexa Fluor 647-conjugated AffiniPure anti-rabbit secondary antibody to anti-Nrf2. Nuclei were labeled with DAPI. White arrows show Nrf2 in nuclei. Representative images are from 12 independent experiments. Scale bars represent 25 μm. Nrf2 levels in KD and OE cells were relative to WT cells (1.0, time = 0) (J). Data for fluorescence intensity per cell represent mean ± SEM from n = 12 (A and B), n = 16 (C–E), n = 10 (F), n = 16 (G and H), and n = 12 (I and J) independent experiments. (***) $P < 0.0005$: significant difference between unheated control and WT cells heated at 40 °C. (###) $P < 0.0005$: significant difference between WT cells and Nrf2 KD or Nrf2 OE cells. Abbreviations used: DAPI, 4′,6-diamidino-2-phenylindole; GCL, gamma cysteine ligase; HO-1, heme oxygenase-1; Hsp, heat shock protein; KD, knockdown; MnSOD, manganese superoxide dismutase; Nrf2, nuclear factor erythroid 2-related factor 2; OE, overexpression; WT, wild type.

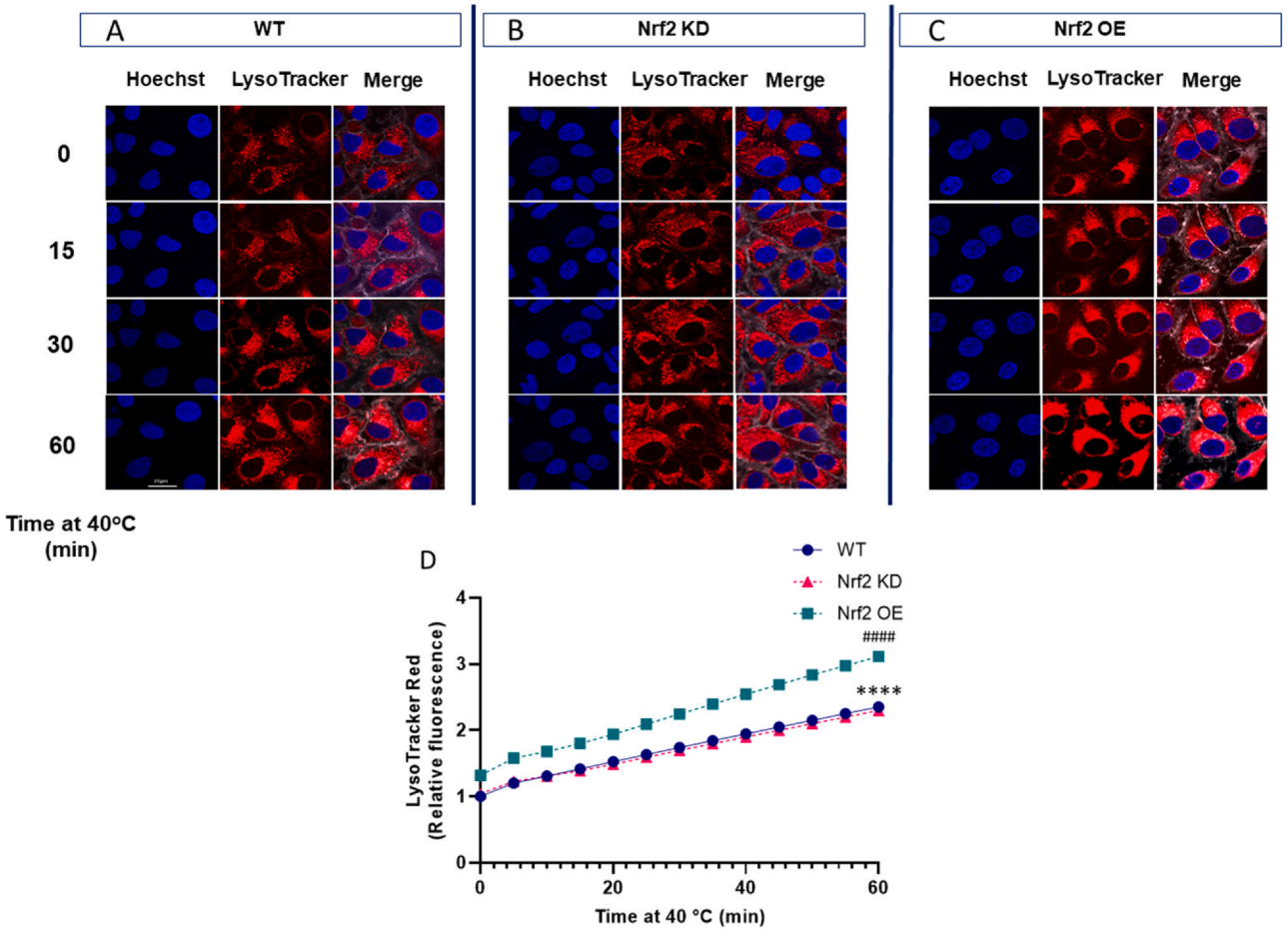

Fig. 4 Acidic vesicular organelle levels increase during mild heat shock at 40 °C. WT cells (A and D) and cells with KD (B and D) or OE (C and D) of Nrf2 were heated at 40 °C from 0 to 60 min, relative to unheated controls (time = 0 min at 40 °C, 1.0). Cells were labeled with Lysotracker red for acidic vesicular organelles and Hoechst 33258 for nuclei (A–C). Representative images (40×) are from 12 independent experiments. Scale bars represent 25 μm. Data for fluorescence intensity per cell represent mean ± SEM from 12 independent experiments (D). Error bars were small and were hidden by the symbols. (****) $P < 0.0001$: significant difference between unheated control and WT cells heated at 40 °C. (####) $P < 0.0001$: significant difference between WT and Nrf2 OE cells. Abbreviations used: KD, knockdown; Nrf2, nuclear factor erythroid 2-related factor 2; OE, overexpression; WT, wild type.

Activation of autophagy by mild heat shock at 40 °C

Autophagy has also been associated with hormesis, although the mechanisms are only starting to be unraveled.[40] We evaluated whether autophagy could be activated as an early cell survival response during a preconditioning heat treatment at 40 °C. Changes in levels of autophagic vacuoles and autophagy proteins were evaluated in cells during heat stress at 40 °C (Figures 4–7).

The levels of acidic vesicular organelles (AVOs) increased significantly in WT cells at 40 °C (Figure 4(A) and (D)). We next determined whether mild heat stress could alter levels of the autophagy protein LC3/Atg8, which is associated with autophagosomes. Western blot analysis showed that mild heat shock at 40 °C significantly increased LC3 II levels by 2-fold in WT cells after 30 and 60 min (Figure 5(A) and (C)). Furthermore, levels of the LC3 I precursor form of the protein increased significantly by 2-fold in WT cells that were heated at 40 °C (Figure 5(B) and (C)). The autophagy protein Beclin-1 (Atg6) is important for the formation of autophagosomes during the initiation stage of autophagy.[41] Heat shock at 40 °C significantly increased protein levels of Beclin-1 by about 1.6-fold after 60 min (Figure 5(D) and (E)).

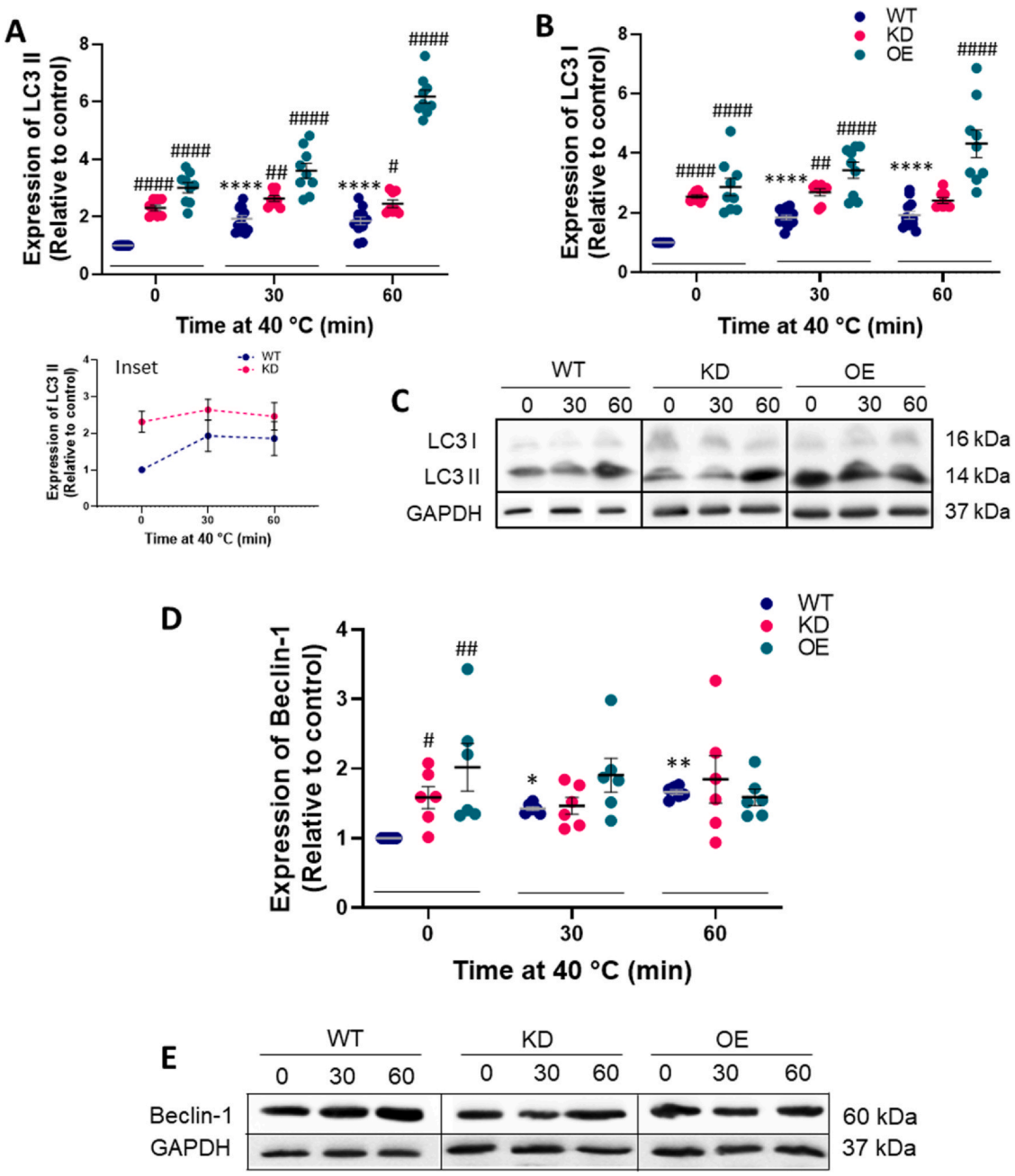

Fig. 5 Mild heat shock at 40 °C increases protein levels of LC3 and Beclin-1. WT cells (blue) and cells with KD (pink) or OE (teal) of nuclear factor erythroid 2-related factor 2 (Nrf2) were heated at 40 °C from 0 to 60 min, relative to unheated controls (time = 0 min at 40 °C, 1.0). Levels of LC3 II, LC3 I (C), and Beclin-1 (E) were detected by Western blotting. Protein expression (30 μg) was normalized to GAPDH loading controls from the same membrane and is relative to unheated controls (WT, time = 0 min, 1.0) (A, B, and D). Representative Western blots are shown. Data represent mean ± SEM from 18 (A), 8 (B), and 6 (D) independent experiments. (*) $P < 0.5$, (**) $P < 0.005$, (***) $P < 0.0005$, or (****) $P < 0.0001$: significant difference between unheated control and cells heated at 40 °C. (#) $P < 0.05$, (##) $P < 0.005$, or (####) $P < 0.0001$: significant difference between WT cells and Nrf2 KD or Nrf2 OE cells for each treatment time. Abbreviations used: GAPDH, glyceraldehyde 3-phosphate dehydrogenase; KD, knockdown; LC3, microtubule-associated protein 1 A/1B-light chain 3; OE, overexpression; WT, wild type.

We explored the effect of mild heat shock at 40 °C on the expression of certain Atg proteins in the two ubiquitin-like conjugating systems.[29] These are the (i) Atg8–LC3--phosphatidylethanolamine and (ii) Atg12–Atg5–Atg16L conjugation systems. For the first system, Atg7 and Atg4B process LC3/Atg8.[42] Protein levels of Atg7 increased significantly by 1.8-fold after 60 min of heating at 40 °C in WT cells (Figure 6(A) and (C)), while heat caused a small

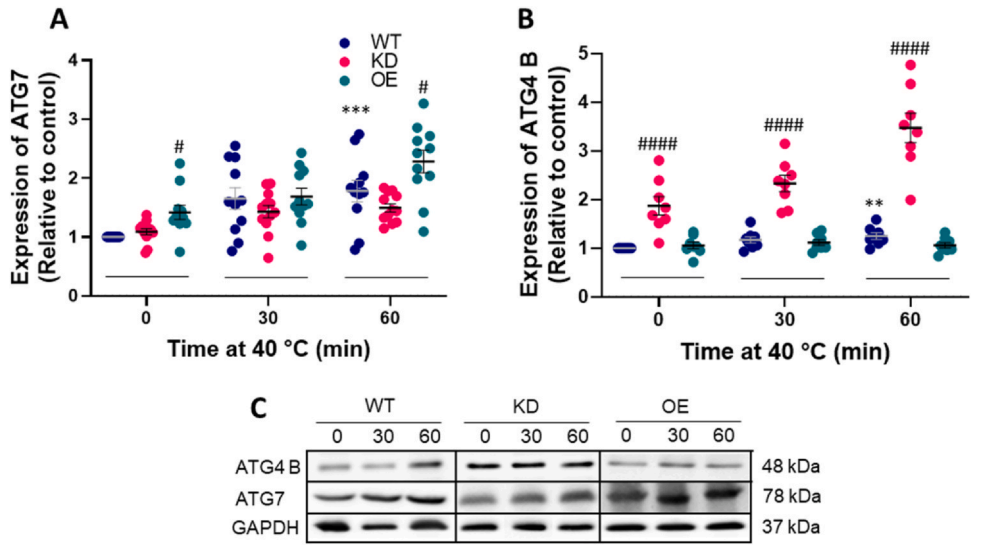

Fig. 6 ATG7 and ATG4B levels increase during heat shock at 40 °C. WT cells (blue) and cells with KD (pink) or OE (teal) of nuclear factor erythroid 2-related factor 2 (Nrf2) were heated at 40 °C from 0 to 60 min, relative to unheated controls (time = 0 min at 40 °C, 1.0). Atg7 (A) and Atg4B (B) were detected by Western blotting (C). Protein expression (30 μg) was normalized to GAPDH loading controls from the same membrane and is relative to unheated controls (WT, time = 0 min, 1.0). Representative Western blots are shown. Data represent mean ± SEM from n = 11 (A) and n = 8 (B) independent experiments. (**) $P < 0.005$ or (***) $P < 0.0005$: significant difference between unheated control and cells heated at 40 °C. (#) $P < 0.05$ or (####) $P < 0.0001$: significant difference between WT cells and Nrf2 KD or Nrf2 OE cells for each treatment time. Abbreviations used: Atg, autophagy-related genes; GAPDH, glyceraldehyde 3-phosphate dehydrogenase; KD, knockdown; OE, overexpression; WT, wild type.

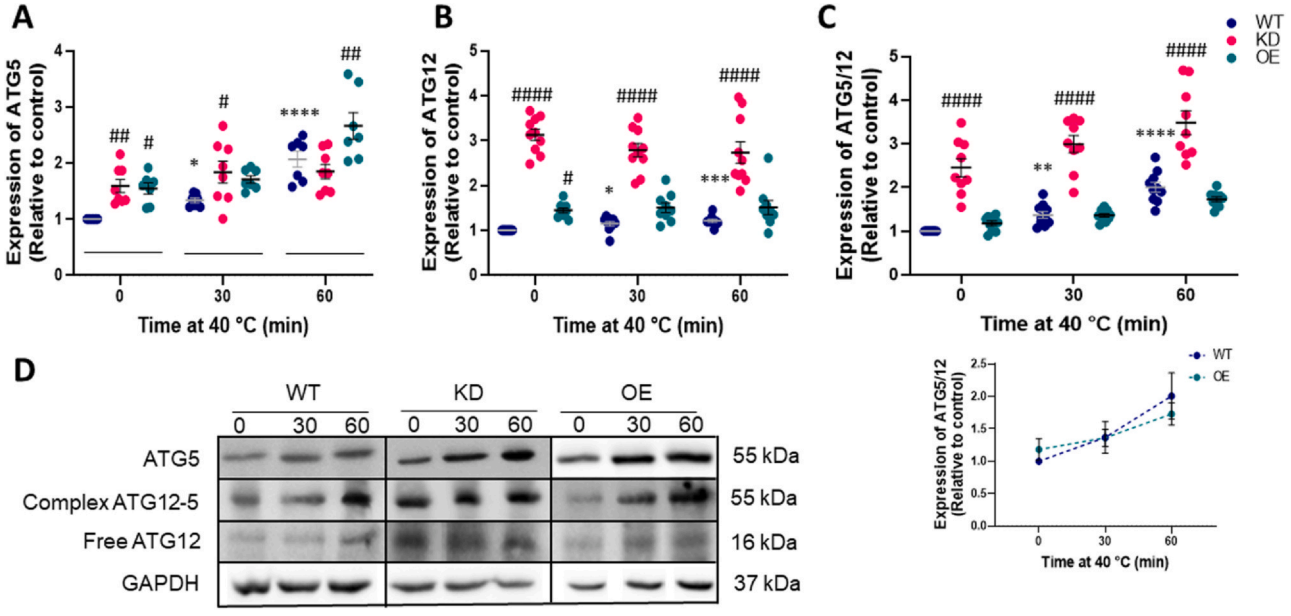

Fig. 7 Mild heat shock at 40 °C increases levels of Atg5 and the Atg12–Atg5 complex. WT cells (blue) and cells with KD (pink) or OE (teal) of nuclear factor erythroid 2-related factor 2 (Nrf2) were heated at 40 °C from 0 to 60 min, relative to unheated controls (time = 0 min at 40 °C, 1.0). Levels of Atg5 (A), Atg12 (B), and the Atg12–Atg5 complex (C) were detected by Western blotting (D). Protein expression (30 μg) was normalized to GAPDH loading controls from the same membrane and is relative to unheated controls (WT, time = 0 min, 1.0). Representative Western blots are shown. Data represent mean ± SEM from n = 7 (A) and n = 9 (B and C) independent experiments. (*) $P < 0.05$, (**) $P < 0.005$, (***) $P < 0.0005$, or (****) $P < 0.0001$: significant difference between unheated control and cells heated at 40 °C. (#) $P < 0.05$, (##) $P < 0.005$, or (####) $P < 0.0001$: significant difference between WT cells and Nrf2 KD or Nrf2 OE cells for each treatment time. Abbreviations used: Atg, autophagy-related genes; GAPDH, glyceraldehyde 3-phosphate dehydrogenase; KD, knockdown; OE, overexpression; WT, wild type.

increase in Atg4B levels by 1.25-fold after 60 min (Figure 6(B) and (C)). For the second conjugation system, Atg5 expression in WT cells increased significantly by 2-fold after 60 min at 40 °C (Figure 7(A) and (D)). There was little change in Atg12 levels at 40 °C (Figure 7(B) and (D)). For the Atg12–Atg5 complex, protein levels increased significantly by 2-fold after 60 min at 40 °C (Figure 7(C) and (D)). Together, these results show that mild heat stress at 40 °C increased levels of autophagy proteins and AVOs.

Role of Nrf2 in activation of autophagy by mild heat shock at 40 °C

To explore whether Nrf2 affected autophagy induction during mild heat shock at 40 °C, the activation of autophagy was evaluated in cells with OE or KD of Nrf2 (Figures 4–8). In Nrf2 KD cells, the significant increase in AVO levels at 40 °C (Figure 4(B) and (D)) was similar to that in WT cells (Figure 4(A) and (D)). Basal levels of AVOs (time = 0) were significantly higher (1.3-fold) in cells with Nrf2 OE (Figure 4(C) and (D)), compared to WT and KD cells (Figure 4(A) and (D)). When Nrf2 OE cells were heated at 40 °C, AVO levels increased significantly during 30 to 60 min (Figure 4(C) and (D)). The increase after 60 min was about 3-fold in OE cells compared to about 2.3-fold in WT and KD cells.

For LC3 II, basal expression in unheated Nrf2 KD cells (time = 0) was significantly higher by 2.3-fold, compared to WT cells (Figure 5(A) and (C)). When Nrf2 KD cells were heated at 40 °C, there was a minor increase in LC3 II levels. In Nrf2 OE cells, there was a significant 3-fold increase in basal levels of LC3 II (time = 0), compared to WT cells (Figure 5(A) and (C)). There was a significant 6-fold increase in LC3 II levels in Nrf2 OE cells after 60 min at 40 °C (Figure 5(A) and (C)). The increase in LC3-II levels in OE cells was much larger than in KD cells during heat stress. Basal levels of LC3 I were significantly higher by 2.5-fold and 2.9-fold, respectively, in unheated cells (time = 0) with either KD or OE of Nrf2, compared to the WT (Figure 5(B) and (C)). A significant 4.3-fold increase in LC3 I levels occurred in Nrf2 OE cells after 60 min at 40 °C, whereas heat did not change LC3 I levels in Nrf2 KD cells. In addition, basal levels of Beclin-1 (time = 0) in cells with either OE or KD of Nrf2 were significantly higher than in the WT (Figure 5(D) and (E)). However, Beclin-1 levels in KD and OE cells did not respond to heat stress at 40 °C.

For the first conjugation system, basal levels of Atg7 (time = 0) in Nrf2 KD cells were similar to those in WT cells and increased significantly by 1.5-fold after 60 min at 40 °C (Figure 6(A) and (C)). For Nrf2 OE cells, basal levels of Atg7 were significantly higher by l.4-fold than the control level (time = 0) and increased significantly by 2.2-fold after 60 min at 40 °C (Figure 6(A) and (C)). In cells with Nrf2 KD, basal levels of Atg4B were significantly higher by 1.9-fold than in wild-type cells (time = 0) (Figure 6(B) and (C)). When Nrf2 KD cells were heated at 40 °C for 60 min, Atg4B levels significantly increased further by 3.5-fold. In Nrf2 OE cells, basal levels of Atg4B were similar to those in WT cells and did not respond to heat stress at 40 °C (Figure 6(B) and (C)).

For the second conjugation system, basal levels (time = 0) of Atg5 in Nrf2 KD cells were significantly higher by 1.6-fold than the WT control (Figure 7(A) and (D)). Atg5 levels increased significantly by 1.8-fold after 60 min of heat shock. Basal levels of Atg5 in Nrf2 OE cells were 1.5-fold higher than WT controls and further increased significantly by 2.7-fold after 60 min at 40 °C (Figure 7(A) and (D)). Basal levels (time = 0) of Atg12 in Nrf2 KD cells were significantly higher by 3.1-fold compared to WT cells and did not change after heating at 40 °C (Figure 7(B) and (D)). In Nrf2 OE cells, basal levels of Atg12 were significantly higher by 1.4-fold than WT controls and were unaffected by heating at 40 °C (Figure 7(B) and (D)). For the Atg12–Atg5 complex, basal levels (time = 0) in Nrf2 KD cells were significantly higher by 2.5-fold than in WT cells and increased significantly by 3.5-fold after 60 min at 40 °C (Figure 7(C) and (D)). In Nrf2 OE cells, basal levels of the Atg12–Atg5 complex were slightly higher than those in WT cells and increased by 2-fold at 40 °C (Figure 7(C) and (D)).

Colocalization of Keap1 and p62

We subsequently determined if heat shock at 40 °C could alter the expression of the Nrf2-sequestering protein Keap1. There was a 1.2-fold increase in Keap1 levels in WT cells after 60 min at 40 °C (Figure 8(A) and (C)). In Nrf2 KD cells, basal levels (time = 0) of Keap1 were significantly higher by 2.3-fold than in WT controls and did not change further after heating at 40 °C (Figure 8(A) and (C)). Basal levels of Keap1 in Nrf2 OE cells (time = 0) were significantly higher by 1.5-fold than those in WT cells and did not respond to heating at 40 °C (Figure 8(A) and (C)). The cellular response of the autophagy receptor protein p62 to mild heat shock was also investigated. The exposure of WT cells to mild heat shock at 40 °C for 30–60 min caused a 1.4–1.6-fold increase in p62 levels (Figure 8(B) and (C)). For Nrf2 KD cells, basal levels (time = 0) of p62 were significantly higher by 2.2-fold than in WT cells and increased

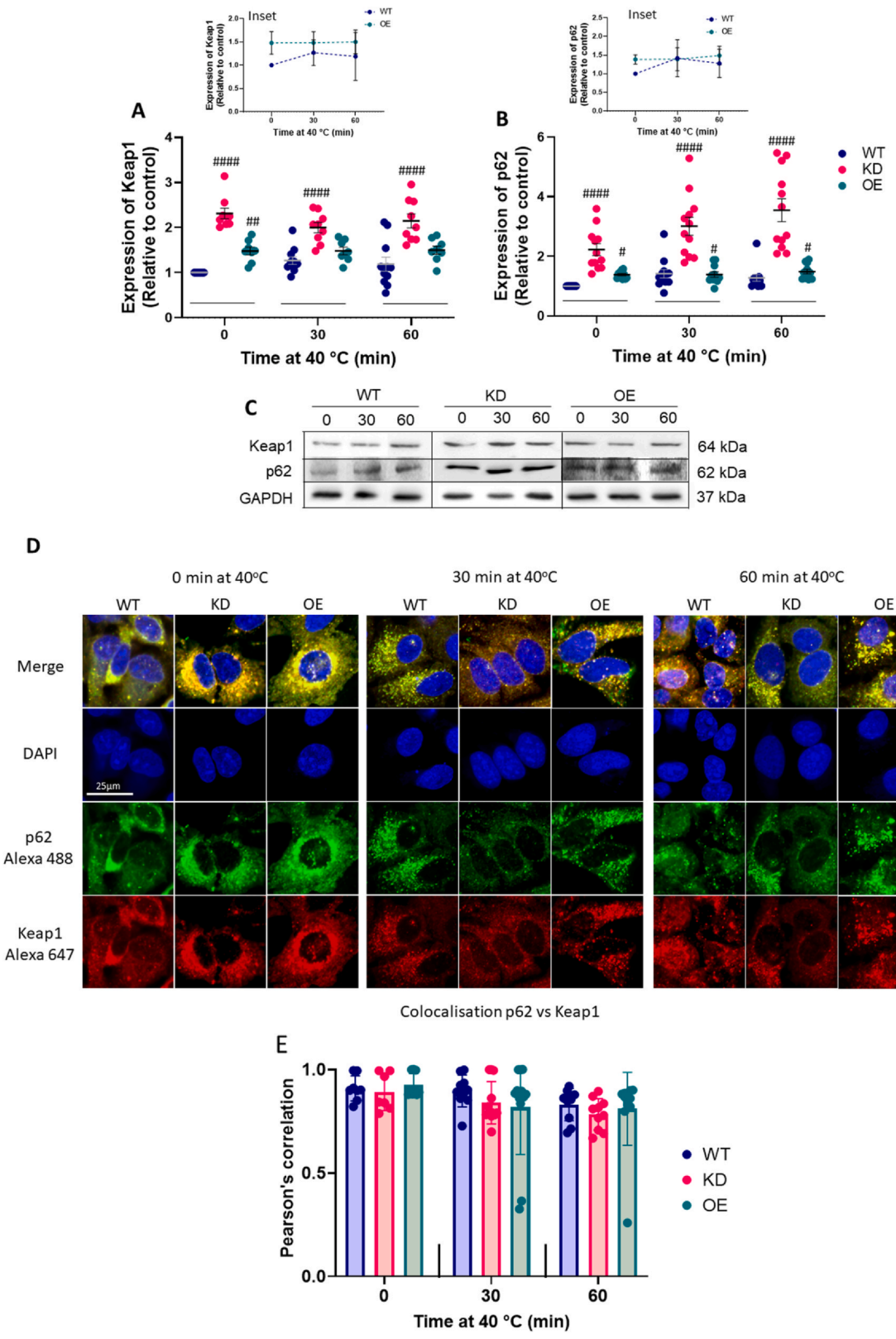
A
Inset
WT
OE
Expression of Keap1 (Relative to control)
Time at 40 °C (min)
####
##
B
Inset
Expression of p62 (Relative to control)
Time at 40 °C (min)
#
WT
KD
OE
C
WT
KD
OE
0 30 60
Keap1
p62
GAPDH
64 kDa
62 kDa
37 kDa
D
0 min at 40°C
30 min at 40°C
60 min at 40°C
Merge
DAPI
25µm
p62 Alexa 488
Keap1 Alexa 647
Colocalisation p62 vs Keap1
E
Pearson's correlation
1.0
0.5
0.0

Fig. 8 Keap1 and p62 levels during heat shock at 40 °C. WT cells (blue) and cells with KD (pink) or OE (teal) of nuclear factor erythroid 2-related factor 2 (Nrf2) were heated at 40 °C from 0 to 60 min, relative to unheated controls (time = 0 min at 40 °C, 1.0). Levels of Keap1 (A) and p62 (B) were detected by Western blotting (C). Protein expression (30 μg) was normalized to GAPDH loading controls from the same membrane and is relative to unheated controls (WT, time = 0 min, 1.0). Representative Western blots are shown. Data represent mean ± SEM from n = 8 (A) and n = 11 (B) independent experiments. (D) Colocalization of fluorescence by confocal microscopy analysis of p62 labeled with Alexa 488 (green fluorescence) and Keap1 labeled with Alexa 647 (red fluorescence) (n = 4) (60×). Nuclei were labeled with DAPI. Colocalization of fluorescence for p62 and Keap1 is shown in yellow. Representative confocal microscope images (magnification 600×): scale bars represent 25 μm. (E) Pearson's correlation for colocalization of p62 and Keap1. (##) $P < 0.005$, (###) $P < 0.0005$, or (####) $P < 0.0001$: significant difference between WT cells and Nrf2 KD or Nrf2 OE cells for each treatment time. Abbreviations used: DAPI, 4′,6-diamidino-2-phenylindole; GAPDH, glyceraldehyde 3-phosphate dehydrogenase; KD, knockdown; Keap1, Kelch ECH associating protein 1; OE, overexpression; WT, wild type.

significantly by 3.5-fold at 40 °C (Figure 8(B) and (C)). Basal levels of p62 were significantly higher by 1.4-fold in Nrf2 OE cells and did not change further when cells were heated at 40 °C (Figure 8(B) and (C)). Analysis by confocal microscope imaging and Pearson correlation revealed colocalization of p62 and Keap1 at time = 0 and following heating at 40 °C for 30–60 min (Figure 8(D) and (E)). Together, these results show that levels of autophagy markers were increased during heat shock at 40 °C. Basal levels of autophagy markers were generally higher in cells with KD or OE of Nrf2.

Discussion

Few studies have examined the induction of autophagy by physiologically relevant and non-lethal temperatures below 41 °C, whereas several studies reported that heat shock increased autophagy at lethal temperatures of 42–47 °C.[43] Our results show that exposure to a mild temperature of 40 °C is non-lethal to cells and constitutes an adaptive survival response induced in response to low-dose stress. Cells that are preconditioned at 40 °C are resistant to cell death induced by exposure to lethal heat shock at 42 °C. This study shows that the exposure of cells to low-dose heat stress at 40 °C for relatively short times of 1–2 h activated autophagy. The activation of autophagy at 40 °C was validated by increased levels of AVOs and the autophagy proteins LC3 II, Beclin-1, Atg7, Atg4B, Atg5, the Atg12–Atg5 complex, and the autophagy receptor protein p62. Macroautophagy consists of five main steps (Figure 9).[29] Beclin-1 binds to the phagophore membrane during the initiation/nucleation step (Figure 9(A)). The two conjugation mechanisms involving (i) LC3-II/Atg4B and Atg7 and (ii) Atg10, Atg7, and Atg5–Atg12–Atg16L are involved in the elongation step (Figure 9(B)). The autophagy receptor p62 forms a complex with LC3-II on the phagophore membrane during elongation (Figure 9(A)). Levels of the transcription factor Nrf2 also increased at 40 °C, and the Nrf2 suppressor protein Keap1 was found to colocalize with p62. Heat shock at 40 °C is a mild, non-cytotoxic stress, and autophagy and Nrf2 were activated as survival responses under these conditions of stress. The importance of these findings is that, during an adaptive survival response induced by mild heat stress at 40 °C, autophagy is induced in addition to multiple cellular defense systems like antioxidants, Hsps, ER stress proteins, and Nrf2.[17,20,33,34] The relative importance of these different defenses during the adaptive survival response is not presently known and requires further investigation.

Studies examining the induction of autophagy by physiologically relevant, non-lethal temperatures under 41 °C are scarce.[43] Core body temperatures above 41 °C are unlikely to be attained in normal human physiology, unless during heat waves, vigorous exercise, or extreme fever. Our results detected cellular and molecular features of autophagy directly after exposure to mild, non-lethal heat shock at 40 °C, without the requirement for a recovery period at 37 °C. In contrast to higher temperatures of 42 °C and above, heat shock at 40 °C does not inhibit protein synthesis.[16] The *ex vivo* heating of whole human blood at mild temperatures of 37 °C, 39 °C, and 41 °C for 90 min caused an increase in autophagic activity in peripheral blood mononuclear cells.[44] In C2C12 mouse myoblasts, there was an increase in autophagy during heating at 40 °C for 60 min[45] Myotubes were returned to 37 °C for a recovery period of 2 or 24 h. The heat caused an increase in phosphocyclic adenosine monophosphate-activated protein kinase (pAMPK) (Thr-172), Beclin-1, and LC3 II, but there was no change in p62. There was a concomitant increase in the heat shock response, shown as upregulation of heat shock factor 1 (HSF1) and Hsp70. These results suggested that a short dose of mild heat at 40 °C could be beneficial to skeletal muscle by increasing 5′ AMP-activated protein kinase activity, markers of autophagosome formation, and the heat shock response.[45]

In *Caenorhabditis elegans*, hormetic heat stress (1 h at 36 °C) or OE of the transcription HSF1 induced autophagy.[46] Under these conditions, autophagy-related

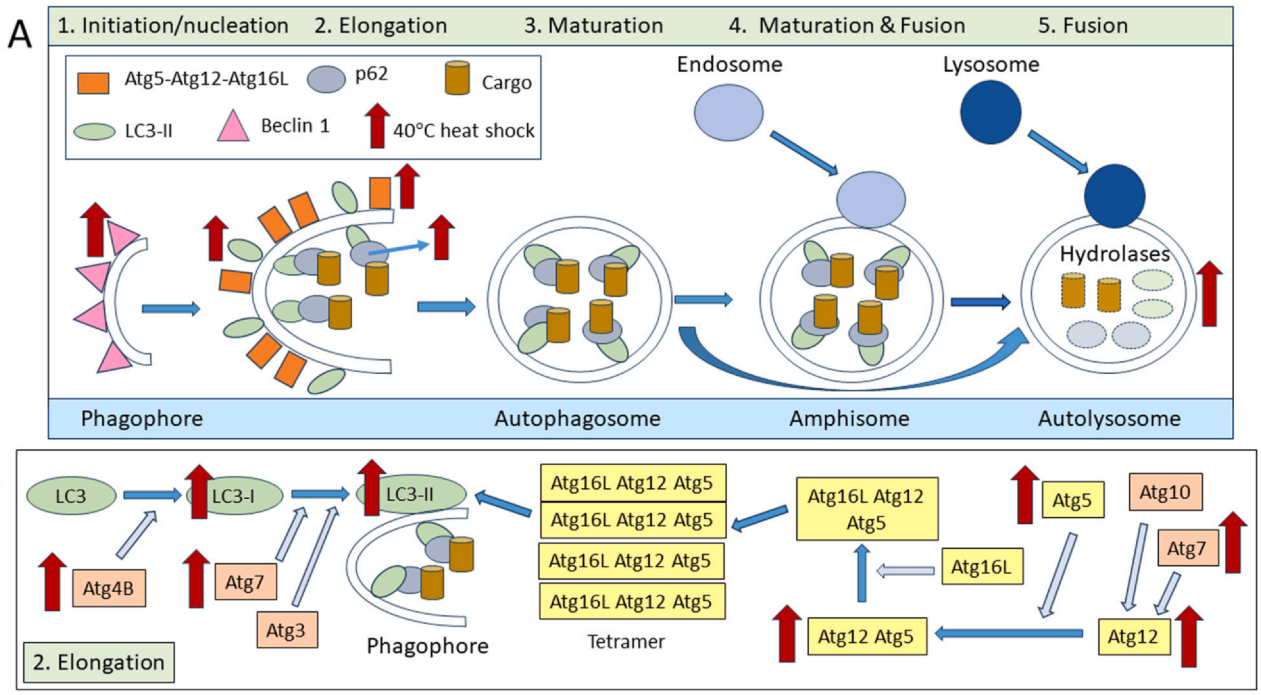

Fig. 9 Activation of autophagy by a mild adaptive survival response induced by mild heat stress at 40 °C. (A) Macroautophagy involves five different steps. 1. During the initiation-nucleation stage, a double-membrane compartment, phagophore, forms in the cytosol. Beclin-1 binds to the phagophore membrane during initiation/nucleation. 2. The elongation stage involves two conjugation systems (B). 3. The closure and maturation steps involve the completion of an autophagosome that encircles cellular content to be eliminated. LC3-II is cleaved from the outer membrane. 4 and 5. Fusion between autophagosomes and endosomes can occur, forming amphisomes, which fuse with lysosomes to form autolysosomes. The final stage is the degradation of cellular material to be eliminated by hydrolases in the acidic environment of lysosomes. (B) For phagophore elongation, two ubiquitin-like conjugating systems are required, involving Atg12–Atg5–Atg16L and LC3-II. Atg4B, Atg7, and Atg3 are essential for the activation of the precursor form of LC3 to produce LC3-II. Atg7 and Atg10 are required for the formation of the Atg12–Atg5–Atg16L tetramer. By binding to LC3-II on the phagophore membrane, p62 selects cellular material (cargo) to be degraded. Red arrows show autophagy molecules that are increased during mild heat shock at 40 °C. Abbreviations used: Atg, autophagy-related genes; LC3, microtubule-associated protein 1 A/1B-light chain 3.

genes were required for thermoresistance and longevity of worms. In addition, hormetic heat stress decreased the accumulation of PolyQ aggregates in an autophagy-dependent manner. Thus, hormetic heat shock improved proteostasis in *C. elegans*. The interplay between the HSF1-mediated heat shock response and autophagy is not well understood, and further studies are required.

Autophagy at higher temperatures

Autophagy is involved in cellular processes such as senescence, development, and immunity.[47] It plays an important role in the turnover of cellular components, including organelles.[48] The induction of autophagy is a complex process that has been shown to involve transcriptional control in the regulation of many additional Atg genes and rapid upregulation of many autophagy-related proteins.[49] Autophagy is generally considered as a survival response that plays a cytoprotective role against a variety of stressors. These include chemical agents (e.g., rapamycin), pro-oxidants (e.g., hydrogen peroxide, menadione), nutrient deprivation, hypoxia, infections, and protein aggregation.[29,50–52] Hence, autophagy functions as a quality control mechanism to maintain cellular homeostasis under conditions of stress.[48] However, higher doses or prolonged exposure to stress can lead to regulated non-apoptotic cell death or autophagy-dependent cell death, which is distinct from apoptosis and necrosis.[29,53,54] The Nomenclature Committee of Cell Death defined autophagy-dependent cell death as "a form of regulated cell death that mechanistically depends on the autophagic machinery (or components thereof)."[55]

Temperature increases of just a few degrees above the physiological level cause protein alterations such as unfolding, entanglement, and unspecific aggregation.[56,57] This leads to disturbances in protein homeostasis. Besides the unfolding of individual proteins, mild heat stress caused the reorganization of actin filaments into stress fibers, leading to disruption of the

cytoskeleton.[57] At higher doses, heat stress caused the collapse of the actin, tubulin, and intermediary networks. Organelles such as the ER and the Golgi undergo fragmentation, while the number of mitochondria decreases.[58] Low-level damage to proteins and organelles at elevated temperatures is an important trigger for activation of autophagy.[59]

At higher, lethal temperatures ranging from 42 to 47 °C, heat shock increased autophagy in different cell types such as hepatocellular carcinoma, human glioma, mouse spermatocytes, embryonic rat heart myoblast H9c2, HeLa, retinal pigment epithelium, lung, and hepatocytes.[60–69] Following high-dose heat shock, activation of autophagy was detected after recovery periods of 2–48 h at 37 °C. Heat shock at these higher temperatures causes a transitory block in protein synthesis for about 2 h.[16] Therefore, increased levels of autophagy proteins would be synthesized after the recovery period at 37 °C. In these studies, autophagy appeared to play a pro-survival role in heat-shocked cells. Autophagy, in addition to Hsps, appears to be essential for cell survival through the clearance of proteins that are irreversibly damaged during high-dose heat shock.[43]

Few studies have looked at upstream cell signaling mechanisms involved in heat-induced autophagy. At high-dose heat shock, activation of AMP-activated protein kinase and inhibition of mammalian target of rapamycin were implicated in autophagy induction in A549 and NCI-H460 lung cells (41–45 °C, 1–2 h)[65] and hepatocellular carcinoma cell lines (SMMC7721 and Huh7) (43–47 °C, 1 h).[66] Levels of adenosine triphosphate (ATP) decreased giving rise to an increase in the AMP:ATP ratio.[66] During heat shock at 43 °C in HeLa cells, aberrantly folded/aggregated proteins caused induction of autophagy by nuclear factor kappa-light-chain-enhancer of activated B cells (NF-κB).[67] However, Bcl-2/Bcl-X_L and the autophagy regulators mammalian target of rapamycin kinase and the Beclin-1/class III PI3K complex were not involved in NF-κB activation during heat shock. To our knowledge, upstream signaling pathways involved in autophagy induction by mild heat shock have not been explored.

Adaptive cell survival (hormetic) responses

Adaptive survival responses are also known as hormesis.[70] A wide variety of chemical compounds and physical agents that incur stress exhibit biphasic dose–response curves, where there is a low dose/concentration stimulation and a high dose/concentration inhibition.[71] This corresponds to a non-cytotoxic preconditioning dose and a higher cytotoxic dose. If the stress is too strong or prolonged, then cells generally die by processes such as apoptosis.

Heat shock also induces a biphasic, hormetic response that occurs in a variety of different cell types. Mild, non-toxic heat stress (40 °C) caused increased levels of cellular defense molecules such as antioxidants[20] and Hsps,[17,21] whereas exposure to higher temperatures (≥42 °C) caused cytotoxicity and cell death.[17,21,33] Our current study shows that mild heat stress at 40 °C increased autophagy markers. It appears that protective factors such as Hsps, antioxidants, and autophagy proteins can act concomitantly to enable cells to continue to function normally despite exposure to stress and cytotoxic aggressions.[52] Metformin, used for the treatment of type 2 diabetes, induced hormetic, adaptive responses in several different cell types including stem cells, hepatocytes, cardiomyocytes, immune cells, adipocytes, and neuronal cells.[70] The mechanism(s) whereby metformin produced protective effects were related to a variety of antioxidants that protected against oxidative stress damage and involved upregulation of Nrf2. Metformin is one example of many compounds that can induce hormetic, adaptive responses. However, much remains to be discovered in an integrated fashion about mechanisms involved in hormetic responses.

Nrf2 and autophagy

The canonical regulation of Nrf2 activity occurs through binding interactions with its cytosolic repressor protein Keap1, which keeps Nrf2 inactive and at low levels by mediating its ubiquitinylation and degradation. Keap1 has two glycine repeat domains (DGR) that are important for inhibition of Nrf2 activity.[22] In response to oxidants, several reactive sensor cysteine residues on Keap1 are modified, leading to a structural change and decreased affinity between Nrf2 and the DGR domains of Keap1.[72] Thus, the binding sites of “inactivated” Keap1 remain occupied with “old” Nrf2. This allows newly synthesized Nrf2 to bypass Keap1, which prevents ubiquitination and degradation of Nrf2. Therefore, Nrf2 accumulates at much higher levels, translocates to the nucleus, and activates ARE-dependent gene expression.

However, Nrf2 can be integrated into the autophagy response pathway in a non-canonical manner through the p62 ubiquitin-binding autophagy receptor protein.[35–37] This mechanism arises through a novel, cysteine sensor-independent mechanism and is not dependent on the cellular redox state. The p62 protein can prevent binding of Nrf2 to the DGR domains of Keap1.[22,35] p62 OE led to a significant decrease in the ubiquitination of Nrf2, resulting in upregulation of

ARE-dependent gene expression.[37] This confirmed that p62 is a competitive inhibitor of Nrf2 binding to Keap1.

p62 contains an ARE, is a target gene of Nrf2, and can be upregulated by Nrf2.[73] In turn, p62 can promote selective Keap1 ubiquitinylation and degradation through autophagy, which leads to prolonged Nrf2 activation and upregulation of the antioxidant response.[24,35,36,38,74] The phosphorylation of p62 at Ser351 markedly increased the binding affinity of p62 for Keap1, leading to the inactivation of Keap1 and release of Nrf2.[75] Persistent Nrf2 activation through the accumulation of phosphorylated p62 contributed to cellular growth in human hepatocellular carcinoma cells.[75] Thus, a p62-Keap1-Nrf2 positive feedback loop is established, which further enhances the protective effects of the Nrf2 and autophagy pathways on cells. However, in general, different studies looked at interactions between the autophagy protein p62 and Nrf2 during stress generated by oxidants. However, the interplay between the Nrf2 and autophagy pathways during other stress conditions, including the heat shock response, remains largely unknown and needs to be explored. In one study, mice were subjected to a 2 h high-dose heat treatment at 42 °C for eight different days.[76] They found that protein expression of both Nrf2 and p62/SQSTM1 increased in Leydig cells.

Nrf2 and autophagy during mild heat stress at 40 °C

Interactions between Nrf2 and autophagy have not been evaluated previously in response to a hormetic, adaptive cell survival response induced by mild heat shock at 40 °C. When Nrf2 levels were depleted in unstressed HeLa cells, there was an increase in basal levels of the autophagy proteins LC3-II, Beclin-1, Atg4B, Atg5, Atg12, the Atg5/12 complex, and p62. These responses involved both Atg conjugation systems, LC3-II and ATG5–Atg12. Basal levels of Atg7 and AVOs in Nrf2 KD cells, however, were not significantly different from levels in WT cells.

In Nrf2-depleted cells, stress induced by mild heat shock at 40 °C caused an increase in AVO levels and further increases in levels of Atg7, Atg4B, Atg5, the Atg5–Atg12 complex, and p62 (Figure 10(A)). The response at 40 °C entailed the Atg12–Atg5 conjugation system, whereas LC3-II did not appear to be involved. Nrf2 is a major cellular defense molecule and when depleted, a huge imbalance in defense systems would be created in cells. When its levels are diminished, activation of autophagy would likely compensate as a defense mechanism to protect cells under both normal conditions and during stress.

Our results show for the first time that protein levels of both Nrf2 and p62 increased during mild heat shock at 40 °C and that colocalization of p62 with Keap1 occurred. Basal levels of p62 were more than 2-fold higher in unstressed Nrf2 KD cells and increased even further during mild heat shock at 40 °C. When Nrf2 levels are low, it is likely that p62 will bind Keap1 to minimize degradation of Nrf2 (Figure 10(A)). Colocalization studies showed that p62 was bound to Keap1 in both unstressed cells and those heated at 40 °C. This would probably allow low-level transcriptional activation of Nrf2 target genes such as catalase, MnSOD, GCL, HO-1, and Hsp72. These results support a role for both the Nrf2 and autophagy pathways in the induction of the adaptive cell survival response at 40 °C.

When Nrf2 was overexpressed in unstressed HeLa cells, there were increases in basal levels of AVOs and the autophagy proteins LC3-II, Beclin-1, Atg7, Atg5, Atg12, and the Atg5–12 complex. Smaller increases occurred for Keap1 and p62.

During mild heat stress at 40 °C, levels of AVOs, LC3-II, Atg7, Atg5, and the Atg5–12 complex increased further in Nrf2-overexpressing cells (Figure 10(A)). The response at 40 °C in Nrf2 OE cells entailed both Atg conjugation systems, LC3-II and Atg12–Atg5. Nrf2 is a regulator of numerous genes, and this includes autophagy gene expression.[77] Besides p62, several other autophagy genes were shown to contain an ARE sequence in their promoter regions. These include unc-51-like autophagy-activating kinases 1/2 (ULK1/2), Atg2B, Atg4C, Atg4D, Atg5, Atg7, Atg9B, Atg10, and Atg16L.[77] Therefore, at higher levels of Nrf2, increased levels of autophagy proteins would be expected. This suggests that, when Nrf2 levels are higher, autophagy and Nrf2 would act concomitantly as defense systems to protect cells against stress.[49]

There was little response of Beclin-1 to heat stress at 40 °C in cells with KD or OE of Nrf2, while LC3-II expression was increased. LC3-II is involved during the elongation of autophagy, while Beclin-1 is involved in a pre-autophagosomal structure in the earlier nucleation step (Figure 9(A) and (B)). Beclin-1 interacts with several different cofactors like Atg14L, activating molecule in Beclin 1-regulated autophagy (Ambra1), UV radiation resistance-associated gene, endophilin B1/Bax-interacting factor 1, and RUN domain Beclin 1 interacting and cysteine-rich domain-containing protein to regulate the lipid kinase vacuolar protein sorting-34 (Vps-34) protein.[29,78] This promotes the formation of Beclin 1–Vps34–Vps153/p150 core complexes, thus inducing autophagy. The anti-apoptotic proteins Bcl-2 and Bcl-X_L can bind to the BH3 domain of Beclin-1 and are negative regulators of Beclin-1 by blocking the pro-autophagic activity of Beclin 1.[78] Autophagy is inhibited by ER-localized Bcl-2, and not by mitochondrial Bcl-2, whereas Bcl-X_L binds to Beclin-1 within mitochondria. These interactions with Beclin-1 can

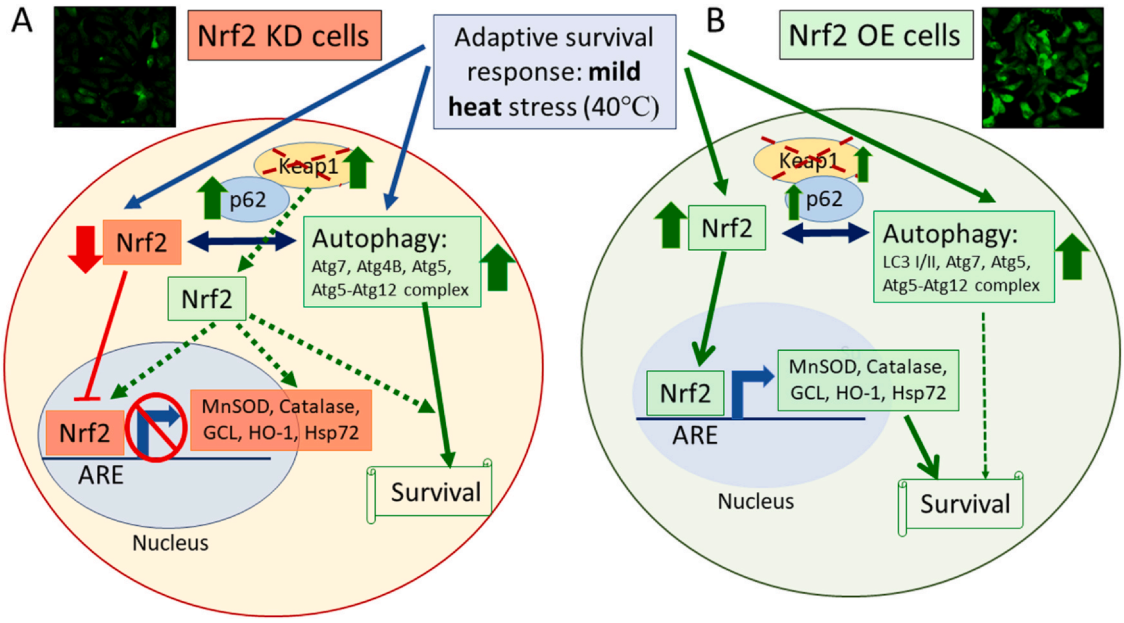

Fig. 10 The adaptive survival response: mild heat stress at 40 °C activates Nrf2 and autophagy. (A). In Nrf2-depleted cells, nuclear translocation of Nrf2 would decrease, and the transcriptional activation of Nrf2 target genes like catalase, MnSOD, HO-1, GCL, and Hsp72 would decrease (Figure 3). However, levels of the autophagy proteins Atg7, Atg4B, Atg5, Atg5–Atg12 complex increased at 40 °C and would likely compensate as a protective mechanism under basal and stress conditions. Further, increased protein expression and colocalization between p62 and Keap1 occurred in Nrf2-depleted cells, which would lead to Keap1 degradation through the autophagy machinery and minimize Nrf2 degradation during mild heat stress at 40 °C. This could allow a low level of Nrf2 accumulation and some transcriptional activation of target genes. (B) When Nrf2 is overexpressed, nuclear translocation of Nrf2 occurs, and the transcriptional activation of Nrf2 target genes like catalase, MnSOD, HO-1, GCL, and Hsp72 is increased (Figure 3). In Nrf2 OE cells, higher levels of autophagy proteins (LC3 I/II, Atg7, Atg5, Atg5–Atg12 complex) from both conjugation systems occurred during mild heat stress at 40 °C, favoring cell survival. Given that Nrf2 levels were high, there were only small increases in p62 and Keap1 levels. This suggests a low level of Keap1 degradation through the autophagy pathway. Cell survival during mild stress would be assured through both the Nrf2 and autophagy pathways. Abbreviations used: ARE, antioxidant response element; Atg, autophagy-related genes; GCL, gamma cysteine ligase; HO-1, heme oxygenase-1; Hsp, heat shock protein; Keap1, Kelch ECH associating protein 1; KD, knockdown; LC3, microtubule-associated protein 1 A/1B-light chain 3; MnSOD, manganese superoxide dismutase; Nrf2, nuclear factor erythroid 2-related factor 2; OE, overexpression.

be disrupted by phosphorylation of Bcl-2 and Bcl-X_L, or ubiquitylation of Bcl-2. We found that mild heat stress at 40 °C increases protein expression of Bcl-2 (unpublished data). Therefore, higher levels of Bcl-2 could block increases in Beclin-1 expression. This idea requires further investigation. Further, it was reported that non-canonical Beclin-1-independent autophagy can occur,[79] and may also explain the lack of heat sensitivity of Beclin-1.

The Keap1-Nrf2-ARE pathway and autophagy are two major intracellular defense systems that protect cells against oxidative stress and other insults to maintain homeostasis. Understanding how Nrf2 and autophagy regulate cell survival is important in neurodegenerative diseases and in cancer.[80] A major dilemma is that Nrf2 and autophagy favor cell survival in both normal and cancerous cells.[72,81] Constitutive activation of Nrf2 through somatic mutations can lead to carcinogenesis and resistance to chemotherapy.[72] Current clinical approaches use Nrf2 inhibitors and Nrf2 lethal anticancer drugs to target tumors.

Our results show that low-dose heat stress at 40 °C increased levels of both Nrf2 and autophagy, which would favor the survival of both normal and tumor cells. For clinical hyperthermia treatments, it would be important to ensure that the entire tumor volume is heated at higher lethal temperatures (> 42 °C) to avoid the induction of increased levels of cellular defenses such as Nrf2 and autophagy by lower heat doses such as 40 °C. However, surrounding normal tissues could be protected against the cytotoxic effects of high-dose heat shock by targeting these areas with low-dose hyperthermia at 40 °C.

Conclusion

The increased understanding of mechanisms underlying cellular responses to low-dose temperatures such as 40 °C is essential for the successful use of hyperthermia in the cancer clinic. Fortunately, resistance to hyperthermia (thermotolerance) induced by preconditioning at low temperatures is a transitory response that usually declines within several days.[16,82]

Therefore, clinical hyperthermia treatments are given at intervals of time to avoid interference due to thermotolerance. In addition, it is important that the entire volumes of solid tumors are thoroughly heated at temperatures that are high enough to destroy all cells. The heating of all tumor cells at lethal temperatures is essential to avoid producing regions of cells that are exposed to mild temperatures, which would render them resistant to adjuvant treatments such as radiation and anticancer drugs, through mechanisms such as the accumulation of Hsps and the activation of autophagy. In another context, the activation of protective survival mechanisms such as autophagy and the heat shock response at low temperatures could offer protection to cells, tissues, and organisms against the adverse effects of a variety of environmental toxins. Further elucidation of the role of cellular stress, autophagy, and cellular survival or death will benefit cancer biology and many other fields.

Materials and methods

Cell culture

Human cervical adenocarcinoma HeLa cells (ATCC no. CCl-2) were used for experiments between passages 7 and 30 and were then restarted from the cryo-freezer. These cells were chosen for the study because cervical cancer responds well to hyperthermia treatments.[1,2] Cells were cultured as monolayers in tissue culture flasks (Sarstedt, St Laurent, QC, Canada) containing Dulbecco modified Eagle's medium (DMEM) (Invitrogen Canada, ThermoFisher Scientific, St Laurent, QC, Canada) with 10% fetal bovine serum (FBS) (Invitrogen Canada), penicillin (50 units/mL), and streptomycin (50 μg/mL) (Hyclone Laboratories, ThermoFisher Scientific). They were maintained in an incubator (Sanyo Scientific, Canada) at 37 °C with a humidified atmosphere of 5% CO_2.[83] The temperature control was ± 0.1 °C and CO_2 control was ± 0.15%. Cell culture medium was replaced with fresh medium 24 h before experiments. Cells were harvested using 0.5 mg/mL trypsin/0.2 mg/mL ethylene diamine tetraacetic acid (EDTA) in phosphate-buffered saline (PBS), washed by centrifugation (1000 × *g*, 3 min), and resuspended for analyses.

Cell lines with overexpression or knockdown expression of Nrf2

Two modified HeLa cells lines were created, one overexpressing the *nrf2* gene and the other with knocked-down expression of the *nrf2* gene, using *nrf2*-specific CRISPR/Cas9 (sc-400017-NIC) and Nrf2 Lentiviral Activation Particles (sc-400017-LAC), as recommended by the manufacturer (Santa Cruz Biotechnology, Dallas, TX, USA). For overexpression of Nrf2 (OE), a synergistic activation mediator transcriptional activation system designed to upregulate gene expression specifically and efficiently *via* lentiviral transduction was used (Santa Cruz Biotechnology). For the KD of Nrf2, a pair of plasmids was designed to knockout gene expression of *nrf2*; each plasmid encoded a D10A-mutated Cas9 nuclease and a target-specific RNA (gRNA) (Santa Cruz Biotechnology). Levels of necrosis (propidium iodide uptake) were very low, between 5% and 7% in all cell types, WT, Nrf2 KD, or Nrf2 OE (data not shown).

Heat treatments

For preconditioning, cells in culture flasks containing culture medium were heated at 40 °C relative to controls (37 °C) for 5–60 min in an incubator at 37–40 °C with a humidified atmosphere of 5% CO_2.[34,84] Cells were then harvested, and cell suspensions were analyzed for levels of AVOs, and protein levels of Nrf2, Keap1, SQSTM1/p62, ATG7, ATG4B, ATG5, ATG12, Beclin-1, and LC3.

To induce thermotolerance, cells confluent at 90% in monolayers in tissue culture flasks containing DMEM medium with 10% FBS were transferred to an incubator with a humidified atmosphere of 5% CO_2 at 40 °C for 3 h, following a period of 20 min to allow culture medium temperature to reach 40 °C.[83] Normal controls were incubated under the same conditions in an incubator at 37 °C. Cells were then harvested and resuspended for analyses, as described above (see Cell culture).

Detection of cell death by flow cytometry

Cells were labeled with the fluorescent probes Annexin V-APC (Invitrogen-ThermoFisher Scientific, St Laurent, QC) and propidium iodide (PI) (Sigma-Aldrich Canada, Oakville, ON). Cells (10^6) in a volume of 100 μL, and were incubated with 5 μL of Annexin V-APC (1/20 dilution) for 10 min, according to the manufacturer's protocol (Invitrogen).[85] Subsequently, 400 μL of DMEM medium containing 5% FBS were added and then 5 μL of PI (final concentration of 2 μM) was added to the cell mixture for 5 min. At least 10,000 cells were analyzed for each sample by flow cytometry at a flow rate of 35 μL/min (BD Accuri™ C6, BD Biosciences, Mississauga, ON). Annexin V-APC was detected using the FL1 channel and PI with the FL3 channel. For this flow cytometer, the pre-optimizing voltage and gain settings do not reduce the fluorescence detection range. Analysis was carried out using BD Accuri™ C6 software. Doublet exclusion was performed by plotting

the height or width against the area for forward scatter or side scatter. Doublets will have double the area and width values of single cells while the height is roughly the same. Therefore, disproportions between height, width, and area can be used to identify doublets (Bio-Rad, flow cytometry guide).

Quantitative reverse transcription polymerase chain reaction (RT-PCR) analysis

Total RNA was isolated from different cells using the Monarch® Total RNA Miniprep Kit (New England Biolabs, Whitby, ON, Canada) according to the manufacturer's instructions. Subsequently, reverse transcription was carried out using the Meridian/Bioline SensiFAST complementary deoxyribonucleic acid (cDNA) Synthesis Kit (FroggaBio Inc, Concord, ON) on a T100 Thermal Cycler (Bio-Rad).

For gene quantification, quantitative PCR (qPCR) was performed on a CFX96 Touch™ Thermal cycler (Bio-Rad) using the Meridian/Bioline SensiFAST SYBR No-ROX Kit (FroggaBio Inc). The qPCR assay employed specific primers for each target gene. The data were exported as Excel files for analysis. The copy number of each target gene was normalized to the 18S ribosomal RNA (rRNA).

Amplification of the target genes was achieved under the following thermal cycling conditions: The quantitative PCR run program consisted of a first step at 95 °C for 5 min followed by 40 cycles of 15 s at 95 °C and 30 s at 58 °C. The target gene transcript level was normalized against the 18S rRNA level. Fold changes of RNA transcripts were calculated using the $2^{-\Delta\Delta Ct}$ method.

Gene	Primer left	Primer right
Nrf2	CGAAACTTTAAAAAGCATTGGA	AGCCCAAATGGTGTCCTAAG
HSP72	TTAGGGGCCTTTCCAAGATT	TTCAACATTGCAAACACAGGA
CAT	CCATTCGATCTCACCAGGGT	GGCCCTGAAGCATTTTGTCA
MnSOD	GGGCACGTGTTAAGGATGTC	CTTCACCGAAAACTCCAGGC
GCL-1	GAGCAACCTACTGTCTAAGCA	TCAGGTCCCAGGTAGTCTTT
HO-1	CCATGAACTTTGTCCGGTGG	GAGAGGGACACAGTGAGAGG
18s	CTTAGAGGGACAAGTGGCG	ACGCTGAGCCAGTCAGTGTA

Abbreviation used: GCL, gamma cysteine ligase; HO-1, heme oxygenase-1; Hsp, heat shock protein; MnSOD, manganese superoxide dismutase; Nrf2, nuclear factor erythroid 2-related factor 2.

Caspase activity

Following heating at 40 or 42 °C for 1–3 h, HeLa cells were harvested and suspended in caspase buffer (10% sucrose, 0.1% 3-[(3-cholamidopropyl) dimethylammonio]-1-propanesulfonate (CHAPS), 20 mM 1,4-piperazinediethanesulfonic acid, 100 mM sodium chloride (NaCl), 10 mM dithiothreitol, 1 mM EDTA, pH 7.2). Cells were then frozen at −80 °C and enzymatic activity was determined in cell lysates using the appropriate substrate (200 μM): Ac-DEVD-7-amino-4-methylcoumarin for caspase-3 and Ac-Leu-Glu-His-Asp-7-amino-4-trifluoromethylcoumarin for caspase-9 (Calbiochem, MilliporeSigma, Sigma-Aldrich Canada).[84,85] The kinetic reactions to generate Ac-Leu-Glu-His-Asp-7-amino-4-trifluoromethylcoumarin (excitation 400 nm, emission 505 nm) or 7-amino-4-methylcoumarin (e.g., 380 nm, em. 460 nm) were detected by spectrofluorometry (Varioskan Lux, ThermoScientific, St Laurent, QC).

Live cell imaging by confocal microscopy

Prior to experiments, 0.2×10^6 cells/mL in DMEM-FBS were plated in a μ-slide 8-well plate for 24 h (ibidi, Fitchburg, WI, USA). For live cell imaging by confocal microscopy, cells in 8-well plates were incubated in a micro-incubator with control of temperature, CO_2, and humidity. Live cell imaging was conducted for 60 min at 40 °C. Cells were then labeled with Hoechst 33258 (25 μg/mL) (Sigma-Aldrich Canada Co.) and 50 nM Lysotracker Red DND 99 (Life Technologies, ThermoFisher Scientific) at 37 °C for 15 min.[86] Cell imaging was conducted with NIS-Element AR4 software using standard excitation and emission filters for visualizing Hoechst 33258 and LysoTracker Red DNP99 using a Confocal inverted microscope Nikon A1+ high sensitivity (cathode GaAsP) (Nikon Canada, Montréal, QC) with either a 40X (Plan Apo λ) or 60X objective (Plan Apo λ, Oil) (Nikon). It is composed of a multispectral detector on 32 channels with resolutions from 2.6 to 10 mm and is equipped with an XY-motorized platinum and piezoelectric system for fast movement in Z-stack. The sample area is scanned at a resolution of 512×512 pixels in 0.6 s. Images were analyzed using FIJI software (NIH, Maryland, USA). Fluorescence intensities were reported per cell and compared between treated and untreated samples. Multiple replicates were performed per experiment, and at least 500 cells were analyzed per condition. Due to variability in the fluorescent signal between experiments, the analysis was consistently referenced to the baseline (zero point) of the normal control condition for accurate analysis and comparison. The temporal trend of each condition remained similar across experiments.

Confocal microscope analysis of fixed cells

Prior to experiments, 0.2×10^6 cells/mL in DMEM-FBS were plated in a μ-slide eight-well plate for 24 h (ibidi). Cells were heated for 5–60 min at 40 °C, then fixed using 3.7% formaldehyde for 15 min in the dark, and then rendered permeable with blocking solution (PBS, 5% bovine serum albumin (BSA), 5% FBS, and 0.1% Triton X-100). Cells were then incubated overnight at 4 °C with primary antibody against Nrf2 (1:200) (MediMabs, Montreal, QC, Canada) in blocking solution followed by a 2 h incubation with Alexa Fluor 647-conjugated AffiniPure anti-rabbit secondary antibody (1:1000) (Jackson Immunoresearch Labs Inc, West Grove, PA, USA) at room temperature. Cell nuclei were labeled with 4′,6-diamidino-2-phenylindole (DAPI) (6.25 μg/mL) during 15 min.[84,86] Cells were rinsed three times with PBS after each incubation procedure. Confocal microscope analysis was conducted as above (section Live cell imaging by confocal microscopy), and standard excitation and emission filters were applied to visualize DAPI and Alexa Fluor 647 (Microscience, Cambridge, MA).

Colocalization of Keap1 and p62 by confocal microscopy

Prior to experiments, 0.2×10^6 cells/mL were plated in a μ-slide 8-well plate for 24 h (ibidi). Cells underwent a heat treatment at 40 °C for 30 and 60 min. Cells were then fixed using 3.7% formaldehyde for 15 min in the dark, and then rendered permeable with blocking solution (PBS, 5% bovine serum albumin (BSA), 5% FBS, and 0.1% Triton X-100). The cells were incubated overnight at 4 °C with a primary antibody against p62 (1:200) (Cell Signaling Technology), followed by a 2 h incubation at room temperature with an Alexa Fluor 488-conjugated anti-rabbit secondary antibody (1:1000) (Jackson Immunoresearch Labs). After washing, cells were then incubated overnight at 4 °C with a primary antibody against Keap1 (1:200) (Cell Signaling Technology). Subsequently, a 2 h incubation at room temperature with an Alexa Fluor 647-conjugated AffiniPure anti-rabbit secondary antibody (1:1000) (Jackson Immunoresearch Labs) was performed. The cells were once again thoroughly washed. To visualize nuclei, DAPI (6.25 μg/mL) was added to the cells for 15 min. The confocal microscope fluorescence analysis was performed as described above (see section Live cell imaging by confocal microscopy), but with filters to visualize DAPI, Alexa Fluor 488 nm, and Alexa Fluor 647 nm with a 60X objective lens (Plan Apo λ, Oil) to capture the images. At least 500 cells were analyzed per image.

Colocalization analysis was performed using the NIS-Element AR4 software. The Pearson's correlation coefficient can be used for quantifying colocalization.[87] Pearson's coefficient, a metric that quantifies the linear correlation between two sets of data, was calculated to evaluate the degree of colocalization between the p62 and Keap1 proteins, indicating the degree of their spatial correlation within the cells. By comparing the Pearson's coefficient values obtained from the control group and the treated group, insights into the spatial relationship and potential interactions between these proteins could be derived. Fluorescence is yellow for colocalization of red and green fluorescence in the merged images.

Western blot analysis

Cells were washed by centrifugation (1000 × *g*, 3 min) in buffer A (100 mM sucrose, 1 mM ethylene glycol tetraacetic acid, 20 mM 3-morpholinopropane-1 sulfonic acid, pH 7.4).[88] The supernatant was discarded, and pelleted cells were resuspended in lysis buffer (20 mM 3-morpholinopropane-1 sulfonic acid, 80 mM β-glycerol phosphate, 10% glycerol, 5 mM ethylene glycol tetraacetic acid, 1 mM EDTA, 2 mM Na_3VO_4, 20 mM $Na_4P_2O_7$, 1 mM NaF, 1 mM dithiothreitol, 1% Triton X-100, pH 7, and a cocktail of protease inhibitors containing 1 mM phenylmethylsulfonyl fluoride, 10 mM aprotinin, 10 μM pepstatin A, 10 μM leupeptin, 25 μM calpain inhibitor (*Complete Mini,* Roche, Millipore Sigma, Etobicoke, ON, Canada)), pH 7.4 and frozen overnight. Following a period of thawing on ice for 30 min with constant vortexing, and a 10 min centrifugation (2500 × *g*), whole cell lysates were collected, removing nuclei and unbroken cells. Proteins were quantified using the Bradford assay (Bio-Rad Laboratories (Canada) Ltd, St Laurent, QC), and 30 μg were separated by sodium dodecyl sulfate-polyacrylamide gel electrophoresis (15%).[89] For Western blotting, proteins were detected using rabbit primary antibodies recognizing Keap1 (D6B12), SQSTM1/p62 (D1Q5S), Atg4B (D1G2R), Atg5 (D5F5U), Atg7 (D12B11), Atg12 (D88H11), LC3A/B (D3U4C) (1:1000), Beclin-1 (D40C5) (1:500) (Cell Signaling Technology Inc) or Nrf2 (1:500) (MediMabs, Montreal, QC, Canada) and horseradish peroxidase-conjugated polyclonal secondary antibody (1:5000). Protein expression was analyzed relative to glyceraldehyde 3-phosphate dehydrogenase (GAPDH) (1:5000) (MediMabs) using a laser scanning densitometer (Fusion Fx7, Montréal Biotech (MBI), Montreal, QC) and Quantity one software (Bio-Rad Laboratories).[83,86] All the Western blots were repeated between 5 and 18 times for each antibody, with N = 2. There

were two different antibodies (e.g., Atg5, Atg12) used per gel (N = 2), followed by a GAPDH loading control. To reprobe for the next antibody, membranes were stripped using 0.2 M glycine at pH 2.2 for 1 h. Each antibody was quantified using the appropriate GAPDH loading control from the same membrane, and the same procedure was used for each of the 5–18 repetitions.

Statistics

Data represent means ± standard error of the mean (SEM) from at least three independent experiments performed in duplicate. Experiments were repeated between five and 18 times, and the number of "n" is indicated in figure legends. Comparisons among multiple groups were made by one-way or two-way analysis of variance (ANOVA), which measures the linear contrast of means. The Bonferroni–Holm adjustment was applied to control for the family-wise error rate at a desired level ($\alpha = 5\%$). The software used was GraphPad Prism5 (GraphPad Software Inc, San Diego, CA, USA). For significant differences, $P < 0.05$.

Author contributions **Diana A. Averill-Bates:** Conceptualization, Methodology, Validation, Resources, Data curation, Writing - review & editing, Visualization, Supervision, Project administration, Funding acquisition. **Claire Chabrol:** Formal analysis, Investigation. **Mélanie Grondin:** Data curation, Methodology, Supervision, Formal analysis, Investigation, Visualization.

Data availability statement Data will be made available on request.

Declarations of interest The authors declare the following financial interests/personal relationships which may be considered as potential competing interests: Diana Averill-Bates reports financial support was provided by the Natural Sciences and Engineering Research Council of Canada. If there are other authors, they declare that they have no known competing financial interests or personal relationships that could have appeared to influence the work reported in this paper.

Acknowledgments The authors thank the Natural Sciences and Engineering Research Council of Canada (#36725-16) (Diana Averill-Bates) for financial support, and Dr Gregoire Bonnamour, Platform manager, and Microscopy and flow cytometry specialist (Université du Québec à Montréal) for assistance with confocal microscope analyses.

References

1. Datta NR, Kok HP, Crezee H, Gaipl US, Bodis S. Integrating loco-regional hyperthermia into the current oncology practice: SWOT and TOWS analyses. *Front Oncol.* 2020;10:819. https://doi.org/10.3389/fonc.2020.00819
2. Van der Zee J. Heating the patient: a promising approach? *Ann Oncol.* 2002;13:1173–1184. https://doi.org/10.1093/annonc/mdf280
3. Baronzio GF, Parmar G, Ballerini M, Szasz A, Baronzio M, Cassutti V. A brief overview of hyperthermia in cancer treatment. *J Integrative Oncol.* 2014;3:1–10. https://doi.org/10.4172/2329-6771.1000115
4. Datta N, Ordóñez SG, Gaipl U, et al. Local hyperthermia combined with radiotherapy and-/or chemotherapy: recent advances and promises for the future. *Cancer Treat Rev.* 2015;41:742–753. https://doi.org/10.1016/j.ctrv.2015.05.009
5. Lutgens LC, Koper PC, Jobsen JJ, et al. Radiation therapy combined with hyperthermia versus cisplatin for locally advanced cervical cancer: results of the randomized RADCHOC trial. *Radiother Oncol.* 2016;120:378–382. https://doi.org/10.1016/j.radonc.2016.02.010
6. Seifert G, Budach V, Keilholz U, Wust P, Eggert A, Ghadjar P. Regional hyperthermia combined with chemotherapy in paediatric, adolescent and young adult patients: current and future perspectives. *Radiat Oncol.* 2016;11:65–72. https://doi.org/10.1186/s13014-016-0639-1
7. Overgaard J. The heat is (still) on–the past and future of hyperthermic radiation oncology. *Radiother Oncol.* 2013;109:185–187. https://doi.org/10.1016/j.radonc.2013.11.004
8. Issels R, Kampmann E, Kanaar R, Lindner LH. Hallmarks of hyperthermia in driving the future of clinical hyperthermia as targeted therapy: translation into clinical application. *Int J Hyperthermia.* 2016;32:89–95. https://doi.org/10.3109/02656736.2015.1119317
9. Van der Zee J, van Rhoon GC. Hyperthermia is effective in improving clinical radiotherapy results. *Int J Radiat Oncol Biol Phys.* 2006;66:633–634. https://doi.org/10.1016/j.ijrobp.2006.05.058
10. Song CW, Park HJ, Lee CK, Griffin R. Implications of increased tumor blood flow and oxygenation caused by mild temperature hyperthermia in tumor treatment. (Review). *Int J Hyperthermia.* 2005;21:761–767. https://doi.org/10.1080/02656730500204487
11. Repasky EA, Evans SS, Dewhirst MW. Temperature matters! And why it should matter to tumor immunologists. *Cancer Immunol Res.* 2013;1:210–216. https://doi.org/10.1158/2326-6066.CIR-13-0118
12. Burchardt E, Roszak A. Hyperthermia in cervical cancer - current status. *Rep Pract Oncol Radiother.* 2018;23:595–603. https://doi.org/10.1016/j.rpor.2018.05.006
13. Bettaieb A, Wrzal PK, Averill-Bates DA. Hyperthermia: cancer treatment and beyond. In: Rangel L, ed. *Cancer Treatment—Conventional and Innovative Approaches.* London: In Tech Open Limited; 2013:257–283. https://doi.org/10.5772/45937
14. Milleron R, Bratton S. 'Heated'debates in apoptosis. *Cell Mol Life Sci.* 2007;64:2329–2333. https://doi.org/10.1007/s00018-007-7135-6
15. Subjeck J, Sciandra J, Johnson R. Heat shock proteins and thermotolerance; a comparison of induction kinetics. *Br J Radiol.* 1982;55:579–584. https://doi.org/10.1259/0007-1285-55-656-579
16. Przybytkowski E, Bates JH, Bates DA, Mackillop WJ. Thermal adaptation in CHO cells at 40 degrees C: the influence of growth conditions and the role of heat shock proteins. *Radiat Res.* 1986;107:317–331.
17. Bettaieb A, Averill-Bates DA. Thermotolerance induced at a fever temperature of 40°C protects cells against hyperthermia-induced apoptosis mediated by death receptor signalling.

Biochem Cell Biol. 2008;86:521–538. https://doi.org/10.1139/O08-136
18. Singh IS, Hasday JD. Fever, hyperthermia and the heat shock response. *Int J Hyperthermia.* 2013;29:423–435. https://doi.org/10.3109/02656736.2013.808766
19. Landry J, Bernier D, Chrétien P, Nicole LM, Tanguay RM, Marceau N. Synthesis and degradation of heat shock proteins during development and decay of thermotolerance. *Cancer Res.* 1982;42:2457–2461.
20. Pallepati P, Averill-Bates DA. Mild thermotolerance induced at 40 degrees C increases antioxidants and protects HeLa cells against mitochondrial apoptosis induced by hydrogen peroxide: role of p53. *Arch Biochem Biophys.* 2010;495:97–111. https://doi.org/10.1016/j.abb.2009.12.014
21. Bettaieb A, Averill-Bates DA. Thermotolerance induced at a mild temperature of 40°C protects cells against heat shock-induced apoptosis. *J Cell Physiol.* 2005;205:47–57. https://doi.org/10.1002/jcp.20386
22. Bellezza I, Giambanco I, Minelli A, Donato R. Nrf2-Keap1 signaling in oxidative and reductive stress. *Biochim Biophys Acta Mol Cell Res.* 2018;1865:721–733. https://doi.org/10.1016/j.bbamcr.2018.02.010
23. Espinosa-Diez C, Miguel V, Mennerich D, et al. Antioxidant responses and cellular adjustments to oxidative stress. *Redox Biol.* 2015;6:183–197. https://doi.org/10.1016/j.redox.2015.07.008
24. Adinolfi S, Patinen T, Deen AJ, et al. The KEAP1-NRF2 pathway: targets for therapy and role in cancer. *Redox Biol.* 2023;63:102726. https://doi.org/10.1016/j.redox.2023.102726
25. Itoh K, Ye P, Matsumiya T, Tanji K, Ozaki T. Emerging functional cross-talk between the Keap1-Nrf2 system and mitochondria. *J Clin Biochem Nutr.* 2015;56:91–97. https://doi.org/10.3164/jcbn.14-134
26. Blank V. Small Maf proteins in mammalian gene control: mere dimerization partners or dynamic transcriptional regulators? *J Mol Biol.* 2008;376:913–925. https://doi.org/10.1016/j.jmb.2007.11.074
27. Lin L, Baehrecke EH. Autophagy, cell death, and cancer. *Mol Cell Oncol.* 2015;2:e985913. https://doi.org/10.4161/23723556.2014.985913
28. Wesselborg S, Stork B. Autophagy signal transduction by ATG proteins: from hierarchies to networks. *Cell Mol Life Sci.* 2015;72:4721–4757. https://doi.org/10.1007/s00018-015-2034-8
29. Redza-Dutordoir M, Averill-Bates DA. Interactions between reactive oxygen species and autophagy. Special Issue: death mechanisms in cellular homeostasis. *Biochim Biophys Acta Mol Cell Res.* 2021;1868:119041. https://doi.org/10.1016/j.bbamcr.2021.119041
30. Klionsky DJ, Codogno P, Cuervo AM, et al. A comprehensive glossary of autophagy-related molecules and processes. *Autophagy.* 2010;6:438–448. https://doi.org/10.4161/auto.6.4.12244
31. Mizushima N. A brief history of autophagy from cell biology to physiology and disease. *Nat Cell Biol.* 2018;20:521–527. https://doi.org/10.1038/s41556-018-0092-5
32. Parzych KR, Klionsky DJ. An overview of autophagy: morphology, mechanism, and regulation. *Antioxid Redox Signal.* 2014;20:460–473. https://doi.org/10.1089/ars.2013.5371
33. Bettaieb A, Averill-Bates DA. Thermotolerance induced at a mild temperature of 40 °C alleviates heat shock-induced ER stress and apoptosis in HeLa cells. *Biochim Biophys Acta Mol Cell Res.* 2015;1853:52–62. https://doi.org/10.1016/j.bbamcr.2014.09.016
34. Glory A, Averill-Bates DA. The antioxidant transcription factor Nrf2 contributes to the protective effect of mild thermotolerance (40°C) against heat shock-induced apoptosis. *Free Radic Biol Med.* 2016;99:485–497. https://doi.org/10.1016/j.freeradbiomed.2016.08.032
35. Komatsu M, Kurokawa H, Waguri S, et al. The selective autophagy substrate p62 activates the stress responsive transcription factor Nrf2 through inactivation of Keap1. *Nat Cell Biol.* 2010;12:213–223. https://doi.org/10.1038/ncb2021
36. Filomeni G, De Zio D, Cecconi F. Oxidative stress and autophagy: the clash between damage and metabolic needs. *Cell Death Differ.* 2015;22:377–388. https://doi.org/10.1038/cdd.2014.150
37. Baird L, Yamamoto M. The molecular mechanisms regulating the KEAP1-NRF2 pathway. *Mol Cell Biol.* 2020;40:e00099-20. https://doi.org/10.1128/MCB.00099-20
38. Taguchi K, Fujikawa N, Komatsu M, et al. Keap1 degradation by autophagy for the maintenance of redox homeostasis. *Proc Natl Acad Sci USA.* 2012;109:13561–13566. https://doi.org/10.1073/pnas.1121572109
39. Calabrese EJ, Kozumbo WJ. The phytoprotective agent sulforaphane prevents inflammatory degenerative diseases and age-related pathologies via Nrf2-mediated hormesis. *Pharmacol Res.* 2021;163:105283. https://doi.org/10.1016/j.phrs.2020.105283
40. Moore MN. Lysosomes, autophagy, and hormesis in cell physiology, pathology, and age-related disease. *Dose Response.* 2020;18:1559325820934227. https://doi.org/10.1177/1559325820934227
41. He C, Levine B. The beclin 1 interactome. *Curr Opin Cell Biol.* 2010;22:140–149. https://doi.org/10.1016/j.ceb.2010.01.001
42. Maruyama T, Noda NN. Autophagy-regulating protease Atg4: structure, function, regulation and inhibition. *J Antibiot.* 2017;71:72–78. https://doi.org/10.1038/ja.2017.104
43. McCormick JJ, Dokladny K, Moseley PL, Kenny GP. Autophagy and heat: a potential role for heat therapy to improve autophagic function in health and disease. *J Appl Physiol.* 2021;130:1–9. https://doi.org/10.1152/japplphysiol.00542.2020
44. McCormick JJ, King KE, Côté MD, et al. Regulation of autophagy following ex vivo heating in peripheral blood mononuclear cells from young adults. *J Therm Biol.* 2020;91:102643. https://doi.org/10.1016/j.jtherbio.2020.102643
45. Summers CM, Valentine RJ. Acute heat exposure alters autophagy signaling in C2C12 myotubes. *Front Physiol.* 2019;10:1521. https://doi.org/10.3389/fphys.2019.01521
46. Kumsta C, Hansen M. Hormetic heat shock and HSF-1 overexpression improve *C. elegans* survival and proteostasis by inducing autophagy. *Autophagy.* 2017;13:1076–1077. https://doi.org/10.1080/15548627.2017.1299313
47. Levine B, Kroemer G. Biological functions of autophagy genes: a disease perspective. *Cell.* 2019;176:11–42. https://doi.org/10.1016/j.cell.2018.09.048
48. Doherty J, Baehrecke EH. Life, death and autophagy. *Nat Cell Biol.* 2018;20:1110–1117. https://doi.org/10.1038/s41556-018-0201-5
49. Reggiori F, Klionsky DJ. Autophagic processes in yeast: mechanism, machinery and regulation. *Genetics.* 2013;194:341–361. https://doi.org/10.1534/genetics.112.149013
50. Kroemer G, Marino G, Levine B. Autophagy and the integrated stress response. *Mol Cell.* 2010;40:280–293. https://doi.org/10.1016/j.molcel.2010.09.023
51. Scherz-Shouval R, Shvets E, Fass E, Shorer H, Gil L, Elazar Z. Reactive oxygen species are essential for autophagy and specifically regulate the activity of Atg4. *EMBO J.* 2007;26:1749–1760. https://doi.org/10.1038/sj.emboj.7601623
52. Zhou DR, Eid R, Boucher E, et al. Stress is an agonist for the induction of programmed cell death: a review. *Biochim*

Biophys Acta Mol Cell Res. 2019;1866:699–712. https://doi.org/10.1016/j.bbamcr.2018.12.001
53. Bialik S, Dasari SK, Kimchi A. Autophagy-dependent cell death - where, how and why a cell eats itself to death. *J Cell Sci.* 2018;131:jcs215152. https://doi.org/10.1242/jcs.215152
54. Denton D, Kumar S. Autophagy-dependent cell death. *Cell Death Differ.* 2019;26:605–616. https://doi.org/10.1038/s41418-018-0252-y
55. Galluzzi L, Vitale I, Aaronson SA, et al. Molecular mechanisms of cell death: recommendations of the Nomenclature Committee on Cell Death 2018. *Cell Death Differ.* 2018;25:486–541. https://doi.org/10.1038/s41418-017-0012-4
56. Lepock JR. How do cells respond to their thermal environment? *Int J Hyperthermia.* 2005;21:681–687. https://doi.org/10.1080/02656730500307298
57. Richter K, Haslbeck M, Buchner J. The heat shock response: life on the verge of death. *Mol Cell.* 2010;40:253–266. https://doi.org/10.1016/j.molcel.2010.10.006
58. Welch WJ, Suhan JP. Cellular and biochemical events in mammalian cells during and after recovery from physiological stress. *J Cell Biol.* 1986;103:2035–2052. https://doi.org/10.1083/jcb.103.5.2035
59. Zhang M, Calderwood SK. Autophagy, protein aggregation and hyperthermia: a mini-review. *Int J Hyperthermia.* 2011;27:409–414. https://doi.org/10.3109/02656736.2011.552087
60. Komata T, Kanzawa T, Nashimoto T, et al. Mild heat shock induces autophagic growth arrest, but not apoptosis in U251-MG and U87-MG human malignant glioma cells. *J Neuro-Oncol.* 2004;68:101–111. https://doi.org/10.1023/b:neon.0000027739.33842.6c
61. Swanlund JM, Kregel KC, Oberley TD. Autophagy following heat stress: the role of aging and protein nitration. *Autophagy.* 2008;4:936–939. https://doi.org/10.4161/auto.6768
62. Zhao Y, Gong S, Shunmei E, Zou J. Induction of macroautophagy by heat. *Mol Biol Rep.* 2009;36:2323–2327. https://doi.org/10.1007/s11033-009-9451-4
63. Zhang M, Jiang M, Bi Y, Zhu H, Zhou Z, Sha J. Autophagy and apoptosis act as partners to induce germ cell death after heat stress in mice. *PLoS One.* 2012;7:e41412. https://doi.org/10.1371/journal.pone.0041412
64. Hsu SF, Chao CM, Huang WT, Lin MT, Cheng BC. Attenuating heat-induced cellular autophagy, apoptosis and damage in H9c2 cardiomyocytes by pre-inducing HSP70 with heat shock preconditioning. *Int J Hyperthermia.* 2013;29:239–247. https://doi.org/10.3109/02656736.2013.777853
65. Xie WY, Zhou XD, Yang J, Chen LX, Ran DH. Inhibition of autophagy enhances heat-induced apoptosis in human non-small cell lung cancer cells through ER stress pathways. *Arch Biochem Biophys.* 2016;607:55–66. https://doi.org/10.1016/j.abb.2016.08.016
66. Jiang J, Chen S, Li K, et al. Targeting autophagy enhances heat stress-induced apoptosis via the ATP-AMPK-mTOR axis for hepatocellular carcinoma. *Int J Hyperthermia.* 2019;36:499–510. https://doi.org/10.1080/02656736.2019
67. Nivon M, Richet E, Codogno P, Arrigo A-P, Kretz-Remy C. Autophagy activation by NFκB is essential for cell survival after heat shock. *Autophagy.* 2009;5:766–783. https://doi.org/10.4161/auto.8788
68. Amirkavei M, Plastino F, Kvanta A, Kaarniranta K, André H, Koskelainen A. Hormetic heat shock enhances autophagy through HSF1 in retinal pigment epithelium cells. *Cells.* 2022;11:1778. https://doi.org/10.3390/cells11111778
69. Okusha Y, Murshid A, Calderwood SK. Proteotoxic stress-induced autophagy is regulated by the NRF2 pathway via extracellular vesicles. *Cell Stress Chaperones.* 2023;28:167–175. https://doi.org/10.1007/s12192-023-01326-z
70. Calabrese EJ, Agathokleous E, Kapoor R, Dhawan G, Kozumbo WJ, Calabrese V. Metformin-enhances resilience via hormesis. *Ageing Res Rev.* 2021;71:101418. https://doi.org/10.1016/j.arr.2021.101418
71. Calabrese EJ, Baldwin LA. Defining hormesis. *Hum Exp Toxicol.* 2002;21:91–97. https://doi.org/10.1191/0960327102ht217oa
72. Suzuki T, Takahashi J, Yamamoto M. Molecular basis of the KEAP1-NRF2 signaling pathway. *Mol Cells.* 2023;46:133–141. https://doi.org/10.14348/molcells.2023.0028
73. Jain A, Lamark T, Sjøttem E, et al. p62/SQSTM1 is a target gene for transcription factor NRF2 and creates a positive feedback loop by inducing antioxidant response element-driven gene transcription. *J Biol Chem.* 2010;285:22576–22591. https://doi.org/10.1074/jbc.M110.118976
74. Liu WJ, Ye L, Huang WF, et al. p62 links the autophagy pathway and the ubiquitin–proteasome system upon ubiquitinated protein degradation. *Cell Mol Biol Lett.* 2016;21:29. https://doi.org/10.1186/s11658-016-0031-z
75. Ichimura Y, Waguri S, Sou YS, et al. Phosphorylation of p62 activates the Keap1-Nrf2 pathway during selective autophagy. *Mol Cells.* 2013;51:618–631. https://doi.org/10.1016/j.molcel.2013.08.003
76. Li Z, Li Y, Zhou X, Dai P, Li C. Autophagy involved in the activation of the Nrf2-antioxidant system in testes of heat-exposed mice. *J Therm Biol.* 2018;71:142–152. https://doi.org/10.1016/j.jtherbio.2017.11.006
77. Pajares M, Jimenez-Moreno N, Garcia-Yague AJ, et al. Transcription factor NFE2L2/NRF2 is a regulator of macroautophagy genes. *Autophagy.* 2016;12:1902–1916. https://doi.org/10.1080/15548627.2016.1208889
78. Kang R, Zeh HJ, Lotze MT, Tang D. The Beclin 1 network regulates autophagy and apoptosis. *Cell Death Differ.* 2011;18:571–580. https://doi.org/10.1038/cdd.2010.191
79. Scarlatti F, Maffei R, Beau I, Codogno P, Ghidoni R. Role of non-canonical Beclin 1-independent autophagy in cell death induced by resveratrol in human breast cancer cells. *Cell Death Differ.* 2008;15:1318–1329. https://doi.org/10.1038/cdd.2008.51
80. Yamamoto M, Kensler TW, Motohashi H. The KEAP1–NRF2 system: a thiol-based sensor–effector apparatus for maintaining redox homeostasis. *Physiol Rev.* 2018;98:1169–1203. https://doi.org/10.1152/physrev.00023.2017
81. Kubisch J, Turei D, Foldvari-Nagy L, et al. Complex regulation of autophagy in cancer–Integrated approaches to discover the networks that hold a double-edged sword. *Semin Cancer Biol.* 2013;23:252–261. https://doi.org/10.1016/j.semcancer.2013.06.009
82. Tanguay RM. Genetic regulation during heat shock and function of heat-shock proteins: a review. *Can J Biochem Cell Biol.* 1983;61:387–394. https://doi.org/10.1139/o83-053
83. Glory A, Bettaieb A, Averill-Bates DA. Mild thermotolerance induced at 40°C protects cells against hyperthermia-induced pro-apoptotic changes in Bcl-2 family proteins. *Int J Hyperthermia.* 2014;30:502–512. https://doi.org/10.3109/02656736.2014.968641
84. Redza-Dutordoir M, Kassis S, Ve H, Grondin M, Averill-Bates DA. Inhibition of autophagy sensitizes cells to hydrogen peroxide-induced apoptosis: protective effect of mild thermotolerance

acquired at 40°C. *Biochim Biophys Acta Mol Cell Res.* 2016;1863: 3050–3064. https://doi.org/10.1016/j.bbamcr.2016.09.015

85. Chow-Shi-Yée M, Grondin M, Ouellet F, Averill-Bates DA. Control of stress-induced apoptosis by freezing tolerance-associated wheat proteins during cryopreservation of rat hepatocytes. *Cell Stress Chaperones.* 2020;25:869–886. https://doi.org/10.1007/s12192-020-01115-y
86. Kassis S, Grondin M, Averill-Bates DA. Heat shock increases levels of reactive oxygen species, autophagy and apoptosis. *Biochim Biophys Acta Mol Cell Res.* 2021;1868:118924. https://doi.org/10.1016/j.bbamcr.2020.118924
87. Dunn KW, Kamocka MM, McDonald JH. A practical guide to evaluating colocalization in biological microscopy. *Am J Physiol Cell Physiol.* 2011;300:C723–C742. https://doi.org/10.1152/ajpcell.00462.2010
88. Samali A, Zhivotovsky B, Jones D, Nagata S, Orrenius S. Apoptosis: cell death defined by caspase activation. *Cell Death Differ.* 1999;6:495–496. https://doi.org/10.1038/sj.cdd.4400520
89. Laemmli UK. Cleavage of structural proteins during the assembly of the head of bacteriophage T4. *Nature.* 1970;227: 680–685. https://doi.org/10.1038/227680a0